The Lipid Metabolites Profile in Patients with Pancreatic Cancer: A Controlled Study of Cancer Tissue Versus Matched Para-Cancer Tissue

Xu Hong
Shanghai Fourth People's Hospital Affiliated to Tongji University School of Medicine
Jian Sun
Shanghai Fourth People's Hospital Affiliated to Tongji University School of Medicine
Ling Zhou
Shanghai Fourth People's Hospital Affiliated to Tongji University School of Medicine
Hui Ying Zhu
Shanghai Fourth People's Hospital Affiliated to Tongji University School of Medicine
De Hua Zhou
Shanghai Fourth People's Hospital Affiliated to Tongji University School of Medicine
Guang Ting Qiu
Shanghai Fourth People's Hospital Affiliated to Tongji University School of Medicine
Ming Cheng
Shanghai Fourth People's Hospital Affiliated to Tongji University School of Medicine
Yang Chen
Shanghai Fourth People's Hospital Affiliated to Tongji University School of Medicine
Hua Yu
Shanghai Fourth People's Hospital Affiliated to Tongji University School of Medicine
Ning Dou
Shanghai Fourth People's Hospital Affiliated to Tongji University School of Medicine
Chen Xiang He
Shanghai Fourth People's Hospital Affiliated to Tongji University School of Medicine
Xin Yu Wang (✉ wang_xinyuvip@163.com)
Shanghai Fourth People's Hospital Affiliated to Tongji University School of Medicine
https://orcid.org/0000-0001-8488-7910

Research

Keywords: Lipidomics, Pancreatic cancer, Laparoscopic pancreaticoduodenectomy, Liomarkers

Posted Date: December 16th, 2020

DOI: https://doi.org/10.21203/rs.3.rs-127782/v1

Abstract

Background and objectives: Most patients with pancreatic cancer were diagnosed at a late stage because identifying pancreatic cancer early was difficult. Therefore, it was of great significance to screen specific biomarkers in early stage of pancreatic cancer. The aim of this study was to demonstrate the profile and characteristics of lipid metabolites in patients with pancreatic cancer and to correlate the expression level of these metabolites with the tumor.

Methods: A total of 9 tissue samples from patients with pancreatic cancer were collected and divided into cancer group and para-cancer group according to different sites. All patients' samples were performed a metabolomics analysis based on Liquid Tandem Chromatography Quadrupole Time of Flight Mass Spectrometry.

Results: PCA based on lipidomics analysis could clearly distribute in different regions. OPLS-DA analysis could filter out the irrelevant variables in metabolites and obtain more reliable information about the intergroup differences of metabolites. The volcano plot was used to visualize all variables with VIP>1 and presented the important variables with $P<0.05$ and $|FC|>2$. Euclidean distance matrix was calculated for the quantitative values of the differential metabolites, and the differential metabolites were clustered by using the full linkage method and heat map was used to demonstrate. The different metabolites of each group were compared and analyzed by radar map, the corresponding ratio of the quantitative value of differential metabolites were calculated. Heatmap of correlation analysis showed the correlation coefficient between different metabolites. Bar plot visualized the variation degree and classification information of metabolites. Bubble plot showed the variation degree, difference significance degree and classification information of metabolites.

Conclusion: The tissue samples of pancreatic cancer had the characteristics of lipidomics, and the difference of lipid metabolites could be used as potential tumor markers of pancreatic cancer.

Introduction

Pancreatic cancer was one of the most common malignancies of the digestive system in China. Although the incidence of pancreatic cancer was not high, it was the seventh leading cause of cancer death[1]. Despite advances in surgical techniques and adjuvant therapy, the approach of mortality to morbidity has not changed over the past 40 years. Furthermore, less than 5 percent of patients with pancreatic cancer had a survival rate of more than 5 years, and even among those who could perform radical resection, the 5-year survival rate was only about 20 percent[2]. J. Ferlay et al. believed that pancreatic cancer would exceed breast cancer as the third leading cause of cancer death in the future[3]. The reason for such a low 5-year survival rate for pancreatic cancer was the lack of specific biomarkers for early diagnosis in clinical practice. Therefore, it was of particular importance to look for diagnostic hallmark of significance for pancreatic cancer.

The pancreas was an important organ for regulating lipid metabolism in the body. Thus, lipids and their metabolites might be used as indicators of health or disease. Lipidomics, proposed by Han in 2003, studied all lipid molecules in the body and their role in the regulation of protein expression and gene expression[4]. It has been reported that lipidomics was widely used in the study of biomarkers for various tumors (such as ovarian cancer, prostate cancer, breast cancer, etc.)[5–7]. Recently, studies have reported that the plasma concentrations of arachidonic acid, lysophosphatidylcholine, phosphatidylcholine (34:2) and phosphatidylethanolamine (26:0) were increased in patients with early pancreatic cancer using lipidomics[8]. Since lipid metabolism was involved in the proliferation of pancreatic cancer cells, the detection of such lipid content in plasma might be helpful for the early diagnosis of pancreatic cancer. However, in pancreatic diseases, especially pancreatic cancer, lipidomics studies of pancreatic tissue samples have not been comprehensive.

Although our previous studies have suggested that differences in serum lipid metabolites might serve as potential biomarkers for early diagnosis of pancreatic cancer[9], tissue samples represented changes in the local environment of the tumor and were less affected by systemic factors. We aimed to investigate the predictive value of the local tissue lipid metabolites profile in patients undergoing radical resection of pancreatic cancer. In this study, the differences of lipid metabolites between tumor tissues and adjacent tissues of 9 patients pancreatic cancer were analyzed and compared by metabonomics, so as to find therapeutic targets for pancreatic cancer.

Methods

All participants signed the informed consent form, which was reviewed and approved by the Clinical Research Ethics Committee of Shanghai Fourth People's Hospital Affiliated to Tongji University School of Medicine (No. 2019057-001).

Patients

In total, 9 patients with pancreatic adenocarcinoma that had been treated and accept surgery at the General Surgery, Shanghai Fourth People's Hospital Affiliated to Tongji University School of Medicine, between October 2018 and March 2019 were enrolled in the study. All the 9 patients with pancreatic cancer were diagnosed by CT or MRI before operation and underwent laparoscopic pancreaticoduodenectomy, and postoperative pathology confirmed ductal adenocarcinoma of the pancreas. The mean age of the patients was 63, with 6 males and 3 females. In the clinical stage, 2 cases were T2N0Mx, 3 cases were T2N1Mx, 3 cases were T2N2Mx, and 1 case was T3N1Mx. Fresh frozen tumor tissues were selected as the experimental group, and adjacent tissues were selected as the control group. The exclusion criteria were for the diagnosis of benign tumors, chronic pancreatitis, combined with other tumors, and the recent 6 months of radiotherapy and chemotherapy.

LC-MS/MS Analysis

The UHPLC separation was carried out using a ExionLC Infinity series UHPLC System (AB Sciex), equipped with a Kinetex C18 column (2.1 * 100 mm, 1.7 μm, Phenomen). The mobile phase consisted of 40% water, 60% acetonitrile, and 10 mmol/L ammonium formate. The mobile phase B consisted of 10% acetonitrile and 90% isopropanol, which was added with 50 mL 10 mmol/L ammonium formate for every 1000 mL mixed solvent. The analysis was carried with elution gradient as follows: 0~12.0 min, 40%~100% B; 12.0~13.5 min, 100% B; 13.5~13.7 min, 100%~40% B; 13.7~18.0 min, 40% B. The column temperature was 55 ℃. The auto-sampler temperature was 6 ℃, and the injection volume was 2 μL (pos) or 2 μL (neg), respectively.

The TripleTOF 5600 mass spectrometer was used for its ability to acquire MS/MS spectra on an information-dependent basis (IDA) during an LC/MS experiment. In this mode, the acquisition software (Analyst TF 1.7, AB Sciex) continuously evaluates the full scan survey MS data as it collects and triggers the acquisition of MS/MS spectra depending on preselected criteria. In each cycle, the most intensive 12 precursor ions with intensity above 100 were chosen for MS/MS at collision energy (CE) of 45 eV (12 MS/MS events with accumulation time of 50 msec each). ESI source conditions were set as following: Gas 1 as 60 psi, Gas 2 as 60 psi, Curtain Gas as 30 psi, Source Temperature as 600 ℃, Declustering potential as 100 V, Ion Spray Voltage Floating (ISVF) as 5000 V or -3800 V in positive or negative modes, respectively.

Data preprocessing and annotation

An in-house program was developed using R for automatic data analysis. The raw data files (wiff format) were converted to files in mzXML format using the ‘msconvert’ program from ProteoWizard (version 3.0.19282).Then, the mzxML files were loaded into Lipid Analyzer for data processing. Peak detection was first applied to the MS1 data. The Cent Wave algorithm in XCMS was used for peak detection, with the MS/MS spectrum, lipid identification was achieved through a spectral match using a MS/MS spectral library.

Statistical analysis

All of figures were performed by SIMCA sofware (version 15.0.2, Sartorius Stedim Data Analytics AB, Umea, Sweden). Statistical analysis of partial data was performed using SPSS software version 23.0 (IBM Corporation, 2015, USA). All continuous variables that followed a normal distribution were showed as the mean ± standard deviation and were compared using the Student’s t-test. A bilateral probability (p) value < 0.05 was considered statistically significant. Pearson method was used to calculate the correlation coefficient of the quantitative value of differential metabolites. All patients performed a metabolomics analysis based on Liquid Tandem Chromatography Quadrupole Time of Flight Mass Spectrometry (LC-QTOFMS).

Results

Principal component analysis

Principal component analysis (PCA) was a statistical method that converts a set of observed possible correlated variables into linearly independent variables (i.e., principal components) through orthogonal transformation. PCA could reveal the internal structure of data and transform a multivariate data set into low-latitude data presented with a small number of principal components (PC). SIMCA software (V15.0.2, Sartorius Stedim Data Analytics AB, Umea, Sweden) was used to conduct Data processing LOG conversion plus center (CTR) formatting process, and then automatic modeling analysis[10]. PCA based on lipidomics analysis could clearly distinguish the difference between pancreatic cancer and adjacent tissues **(Figure 1**). The lipid metabolism of the two groups was obviously distributed in different regions, indicating that the lipid metabolism of the two groups had their own unique characteristics. The X-coordinate PC[1] and Y-coordinate PC[2] represented the scores of the first and second PC respectively, and the color and shape of scatter points represented samples experimental grouping. The samples were all within the 95% confidence interval (Hotelling's T-Squared Ellipse).

Orthogonal projections to latent structures - discriminant analysis

In high-dimensional data, variables contained not only differential variables related to categorical variables, but also a large number of undifferentiated variables that may be related to each other. The difference variables would be dispersed to more principal components because of the influence of related variables, so better visualization and subsequent analysis could not be carried out. Orthogonal projections to latent structures - discriminant analysis (OPLS-DA) could filter out orthogonal variables unrelated to categorical variables in metabolites, and analyzed non-orthogonal variables and orthogonal variables respectively, so as to obtain more reliable information about the intergroup differences of metabolites and the degree of correlation between the experimental group. SIMCA software (V15.0.2, Sartorius Stedim Data Analytics AB, Umea, Sweden) was used to perform LOG conversion and UV formatting on the Data. First, OPLS-DA modeling analysis was performed on the first principal component, and 7-fold cross validation was used to verify the quality of the model. Then the validity of the model was evaluated by R2Y (the model's interpretability to the categorical variable Y) and Q^2 (the model's predictability) obtained after cross-validation. Finally, the permutation test was used to randomly change the arrangement order of the classification variable Y for several times to obtain different random Q^2 values, and further tested the validity of the model. To investigate the statistical differences in lipid metabolites between the pancreatic cancer group and the para-cancer group, a multivariate analysis model OPLS-DA was used. Data from the pancreatic group and the para-cancer group were distributed in two opposite regions in the OPLS-DA model analysis (**Figure 2A**). In the figure, the X-coordinate T [1]P represented the predicted principal component score of the first principal component, the Y-coordinate T [1]O represented the orthogonal principal component score, and the shape and color of scatter points represented different experimental groups. The results of the OPLS-DA score chart showed that the two groups of samples differed significantly. All samples were within the 95% confidence interval (Hotelling's T-Squared Ellipse).

The permutation test established the corresponding OPLS-DA model to obtain the R^2 and Q^2 values of the random model by randomly changing the ranking order of the categorical variable Y for several times,

which played an important role in avoiding the overfitting of the test model and evaluating the statistical significance of the model. Q^2 values of the random model were all smaller than Q^2 values of the original model. The intercept of Q^2 regression line and vertical axis was less than zero; at the same time, as the retention degree of displacement decreased gradually, the proportion of Y variable of displacement increased, and Q^2 of the random model decreased gradually. This indicated that the original model had good robustness. The original model could better explain the difference between the two groups of samples **(Figure 2B)**. The abscissa represented the permutation retention of the permutation test (the proportion consistent with the original model's Y variables; the point at which the permutation retention was equal to 1 was the value of R2Y and Q2 of the original model). The vertical coordinate represented the value of R2Y or Q2, the green dot represented the value of R2Y obtained by the permutation test, the blue square represented the value of Q2 obtained by the permutation test, and the two dotted lines represented the regression lines of R2Y and Q2 respectively. The original model R2Y was very close to 1, indicating that the established model conformed to the real situation of the sample data. The original model Q2 was close to 1, indicating that if new samples were added to the model, a more approximate distribution could be obtained. In general, the original model could better explain the difference between the two groups of samples. Q2 values of the random model were all smaller than Q2 values of the original model. The intercept of Q2 regression line and vertical axis was less than zero. At the same time, as the retention degree of displacement decreased gradually, the proportion of Y variable of displacement increased, and Q2 of the random model decreased gradually. This indicated that the original model had good robustness and no overfitting phenomenon exists.

Univariate analysis

Student's t-test P value was less than 0.05, fold change was greater than 2 and variable importance in the projection (VIP) of the first principal component of the OPLS-DA model was greater than 1 when the differential metabolites from the cancer group and the para-cancer group were selected.

Volcano plot

The results of screening differential metabolites in the cancer group versus para-cancer group were visualized in the form of a volcano plot **(Figure 3)**. Each point in the volcano plot represented a metabolite, the horizontal coordinate represents the fold change (FC) of each substance in the comparison group (log2 FC), the vertical coordinate represented the P-value of the Student t test (-log10 P-value), and the size of scatter point represented the VIP value of the OPLS-DA model. The larger the size of scatter point was, the greater the VIP value was. The scatter color represented the final screening result. The significantly up-regulated metabolites were shown in red, the significantly down-regulated metabolites were shown in blue, and the non-significantly different metabolites were shown in gray.

Heat map of hierarchical clustering analysis

Euclidean distance matrix was calculated for the quantitative values of the differential metabolites, and the differential metabolites were clustered by using the full chain method, and the heat map was used to

demonstrate **(Figure 4)**. The abscissa in the figure represented different experimental groups, the ordinate represented the different metabolites compared in this group, and the color blocks at different positions represented the relative expressions of metabolites at corresponding positions.

Radar chart

We calculated the corresponding ratio of the quantitative value of differential metabolites, and took the logarithmic transformation of base 2, which was shown in red in the figure, and the corresponding content trend change was displayed in the radar chart **(Figure 5)**.

Heatmap of correlation analysis

For each group of comparison between the cancer group and the para-cancer group, we calculated the correlation coefficient of the quantitative value of the different metabolites. Pearson's method was used for calculation, and it was presented in the form of headmap **(Figure 6)**. The horizontal and vertical coordinates in the figure represented the different metabolites compared in this group, the color blocks at different positions represented the correlation coefficient between metabolites at corresponding positions, red represented positive correlation and blue represented negative correlation. At the same time, the nonsignificant correlation was marked with a cross.

Bar plot

The bar plot of lipid group visualized the results of cancer group and para-cancer group by using the change degree of metabolite content and classification information **(Figure 7)**. Each column in the lipid column represented a class of metabolites. The ordinate of the figure represented the relative change percentage of the content of various substances in this group ratio. If the relative change percentage of content was 0, it meant that the content of this substance was the same in both groups. The percentage change in relative content was positive, it indicated that the content of this substance was higher in the cancer group. A negative percentage of the relative change in content indicated a higher content of the substance in the para-cancer group. The abscissa of the column chart of lipid group represented the lipid classification information.

Bubble plot

The bubble plot was visualized by the degree of metabolite content change, difference significance and classification information of the cancer group and the para-cancer group **(Figure 8)**. Each point in the bubble represented a metabolite. The size of the point represented the P-value of the student's T-test (-log10 P-value). The bigger the dot, the smaller the p-value. Gray points represented non-significant differences with a P-value not less than 0.05, and colored points represented the p-value was less than 0.05 (different colors marked according to lipid classification). The abscissa of the bubble plot represented the relative change percentage of the content of each substance in the group (for substances with great change in content, the relative change percentage of the content of other substances was marked on the corresponding abscissa scale). The relative change percentage of the content was 0,

indicating the same content of the substance in the two groups. The relative change percentage of content was positive, indicating that the content of this substance was higher in the cancer group. A negative percentage change in relative content indicated a higher content of the substance in the para-cancer group. The ordinate of the bubble plot represented the lipid classification information. The black line at the bottom showed the distribution density of the metabolite (a line represented a metabolite).

Discussion

The insidious onset, inconspicuous early symptoms, rapid progression and high fatality rate of pancreatic cancer brought great difficulties to the early detection, diagnosis and treatment of pancreatic cancer[11]. Although CA199 played an important role in the diagnosis of pancreatic diseases, it was less sensitive to early pancreatic cancer and precancerous lesions. CA199 did not serve as a biomarker for the screening of asymptomatic population, but only for the screening of symptomatic patients or clinical differential diagnosis of other diseases[12]. Therefore, finding specific biomarkers for pancreatic cancer has been a hot topic in pancreatic cancer research.

Lipids were not only involved in the regulation of a variety of life processes, including energy conversion, material transport, information recognition and transmission, etc., but abnormal lipid metabolism was also closely related to some diseases, such as diabetes, Alzheimer's disease (AD) and the occurrence and development of tumors[13–15]. With the development of fast and high-throughput analytical techniques, especially the extensive application of liquid chromatography tandem mass spectrometry (LC-MS/MS) technology, the robust analysis of various trace lipids in samples was achieved through rapid, high-throughput and high-precision analysis, large-scale and comprehensive lipid analysis, as well as metabolic and functional research[16]. Conventional analytical methods included PCA, OPLS-DA, etc[17].

The pancreas was an important organ of lipid metabolism in human body and the study of lipid omics could help to understand the changes of pancreas function. It is reported that the concentration of arachidonic acid, lysophosphatidylcholine, phosphatidylcholine (PC) and phosphatidyl ethanolamine (PE) in the plasma of patients with early pancreatic cancer was found to be increased by the method of lipid group analysis[8, 9]. However, lipid metabolites with differences in pancreatic cancer and adjacent tissues were screened out through tissue samples, and the results showed that PC, PE were significantly increased in cancer tissues, which was basically consistent with previous plasma studies.

PC and PE all belonged to glycerolipids, whichwere the main components on the surface of cell membranes and organelles. For tumor cells, endogenous lipid synthesis not only provided energy for the proliferation of tumor cells, but also provided lipid components of the cell membrane for the proliferation of tumor cells. Studies have shown that the expression of PC and PE in serum of liver cancer patients was different in different TNM stages by LC-MS analysis[18]. Our study showed that the content of PC and PE in pancreatic cancer tissues was higher than that in para-cancer tissues. This also confirmed that glycerolipids including PC and PE played an important role in the development of tumors. At the same

time, our study also further demonstrated that PC and PE could be used as potential biomarkers for tumors.

Tumor cells exhibited metabolic plasticity, providing a selective advantage for tumor cells to survive and proliferate in harsh microenvironments such as hypoxia, acidosis, and malnutrition. In this microenvironment, tumor cell lipid synthesis increased[19]. It has been reported that changes in tumor metabolism and accumulation of metabolites could lead to local immunosuppression in tumor microenvironment. The correlation analysis between the proportion of immune cells and the expression of lipid metabolism genes in tumor microenvironment showed that there were differences in the expression of immune-related lipid metabolism genes, suggesting a potential interaction between lipid metabolism and immune response[20]. Our previous study suggested abnormal lipid metabolism in the serum of pancreatic cancer, and this study further verified this study through tissue samples, which laid a foundation for the later study on the molecular mechanism of lipid metabolism and pancreatic cancer[9].

There was a certain relationship between lipid metabolism and inflammatory reaction. Lipid metabolism disorder could enhance oxidative stress and affect chronic inflammatory reaction. Since inflammatory cytokines tended to be synthesized from activated macrophages and these cells did exist in fat cells in cancer patients with weight loss, immune cells or fat cells might be involved in regulating energy pathways and lipid mobilization. In adipocytes, TNF-γ inhibited lipoprotein lipase activity, resulting in triglyceride uptake and reduced lipid deposition, leading to cachexia. Abnormal lipid metabolism was closely related to digestive tract tumors, especially colorectal cancer[19, 21, 22]. Hyperlipidemia and obesity were high risk factors for colorectal cancer. The increased level of free fatty acids in serum might be related to the occurrence of oxidative stress and the enhancement of lipid toxicity[23]. Currently, the effects on dyslipidemia associated tumorigenesis, transfer mechanism was not clear, so the need for more in-depth research, to explore new targets for cancer treatment. Therefore, it was a new therapeutic idea to explore the therapeutic target of pancreatic cancer by analyzing the abnormal lipid metabolite spectrum.

The advantage of this study was that the most complete analysis of lipid metabolites was performed on tissue samples from patients with pancreatic cancer. The study also had some limitations. We need to further study the molecular mechanism of lipid metabolites and the occurrence and progress of pancreatic cancer. Comparative analysis of pancreatic tissue samples from pancreatic cancer tissues, para-cancer, and healthy controls was also lacking. Further prospective studies and analyses with larger sample sizes are needed to confirm these clinical predictors. Further prospective studies and larger sample size analysis are needed to identify these associated lipid metabolites.

Conclusions

The tissue samples of pancreatic cancer had the characteristics of lipidomics, and the difference of lipid metabolites could be used as potential tumor markers of pancreatic cancer.

Declarations

Acknowledgements

The authors have no conflicts of interest or financial ties to disclose. The authors would like to thank Prof. Xiangdong Wang, Shanghai Zhongshan Hosiptal for her guidance on the design of the study.

Authors' contributions

Xin Yu Wang designed the research; Hong Xu performed the research; Hui Ying Zhu, De Hua Zhou, Guang Ting Qiu, Ming Cheng, Yang Chen, Hua Yu, Ning Dou and Chen Xiang He analyzed the data; Jian Sun and Ling Zhou wrote the paper. The author(s) read and approved the final manuscript.

Funding

Research reported in this publication was supported by grant number SY-XKZT-2019-1006 from Shanghai Fourth People's Hospital Affiliated to Tongji University School of Medicine Discipline Boosting Plan. It was funded primarily in the design of the study and collection, analysis, and interpretation of data and in writing the manuscript.

Availability of data and materials

Access to the database may be obtained from the corresponding author on reasonable request.

Ethics approval and consent to participate

The protocol of this study was approved by the Institutional Review Board of Shanghai Fourth People's Hospital Affiliated to Tongji University School of Medicine (No.2019057-001).

Consent for publication

All participants gave their consent for evaluation and publishing.

Competing interests

The authors declare no conflict of interest.

Author details

[1]Department of General Surgery, Shanghai Fourth People's Hospital Affiliated to Tongji University School of Medicine, No. 1279 Sanmen Road, 200434 Shanghai, China. [2]Department of Neurosurgery, Shanghai Fourth People's Hospital Affiliated to Tongji University School of Medicine, No. 1279 Sanmen Road, 200434 Shanghai, China. [3]These authors contributed equally.

References

1. Bray F, Ferlay J, Soerjomataram I, Siegel RL, Torre LA, Jemal A. Global cancer statistics 2018: GLOBOCAN estimates of incidence and mortality worldwide for 36 cancers in 185 countries. CA Cancer J Clin. 2018;68:394–424.
2. Conroy T, Bachet JB, Ayav A, Huguet F, Lambert A, Caramella C, Maréchal R, Van Laethem JL, Ducreux M. Current standards and new innovative approaches for treatment of pancreatic cancer. Eur J Cancer. 2016;57:10–22.
3. Ferlay J, Partensky C, Bray F. More deaths from pancreatic cancer than breast cancer in the EU by 2017. Acta Oncol. 2016;55:1158–60.
4. Han X, Gross RW. Global analyses of cellular lipidomes directly from crude extracts of biological samples by ESI mass spectrometry: a bridge to lipidomics. J Lipid Res. 2003;44:1071–9.
5. Liu Y, Chen Y, Momin A, Shaner R, Wang E, Bowen NJ, Matyunina LV, Walker LD, McDonald JF, Sullards MC, Merrill AH Jr. Elevation of sulfatides in ovarian cancer: an integrated transcriptomic and lipidomic analysis including tissue-imaging mass spectrometry. Mol Cancer. 2010;9:186.
6. Eberlin LS, Dill AL, Costa AB, Ifa DR, Cheng L, Masterson T, Koch M, Ratliff TL, Cooks RG. Cholesterol sulfate imaging in human prostate cancer tissue by desorption electrospray ionization mass spectrometry. Anal Chem. 2010;82:3430–4.
7. Min HK, Lim S, Chung BC, Moon MH. Shotgun lipidomics for candidate biomarkers of urinary phospholipids in prostate cancer. Anal Bioanal Chem. 2011;399:823–30.
8. Urayama S, Zou W, Brooks K, Tolstikov V. Comprehensive mass spectrometry based metabolic profiling of blood plasma reveals potent discriminatory classifiers of pancreatic cancer. Rapid Commun Mass Spectrom. 2010;24:613–20.
9. Zhou D, Mu D, Cheng M, Dou Y, Zhang X, Feng Z, Qiu G, Yu H, Chen Y, Xu H, Sun J, Zhou L. Differences in lipidomics may be potential biomarkers for early diagnosis of pancreatic cancer. Acta Cir Bras. 2020;35:e202000508.
10. Wiklund S, Johansson E, Sjöström L, Mellerowicz EJ, Edlund U, Shockcor JP, Gottfries J, Moritz T, Trygg J. Visualization of GC/TOF-MS-based metabolomics data for identification of biochemically interesting compounds using OPLS class models. Anal Chem. 2008;80:115–22.
11. Kleeff J, Korc M, Apte M, La Vecchia C, Johnson CD, Biankin AV, Neale RE, Tempero M, Tuveson DA, Hruban RH, Neoptolemos JP. Pancreatic cancer. Nat Rev Dis Primers. 2016;2:16022.
12. Jelski W, Mroczko B. Biochemical diagnostics of pancreatic cancer - Present and future. Clin Chim Acta. 2019;498:47–51.
13. Meyer zu Heringdorf D,Jakobs KH. Lysophospholipid receptors: signalling, pharmacology and regulation by lysophospholipid metabolism. Biochim Biophys Acta. 2007;1768:923–40.
14. Brinkmann V. Sphingosine 1-phosphate receptors in health and disease: mechanistic insights from gene deletion studies and reverse pharmacology. Pharmacol Ther. 2007;115:84–105.
15. Iessi E, Marconi M, Manganelli V, Sorice M, Malorni W, Garofalo T, Matarrese P. On the role of sphingolipids in cell survival and death. Int Rev Cell Mol Biol. 2020;351:149–95.

16. Han X, Gross RW. Shotgun lipidomics: electrospray ionization mass spectrometric analysis and quantitation of cellular lipidomes directly from crude extracts of biological samples. Mass Spectrom Rev. 2005;24:367–412.
17. Putri SP, Yamamoto S, Tsugawa H, Fukusaki E. Current metabolomics: technological advances. J Biosci Bioeng. 2013;116:9–16.
18. Wang W, Lv J, Chen N, Lou B, Mao W, Wang P, Chen Y. Dysregulated serum metabolites in staging of hepatocellular carcinoma. Clin Biochem. 2018;61:7–11.
19. Corbet C, Feron O. Emerging roles of lipid metabolism in cancer progression. Curr Opin Clin Nutr Metab Care. 2017;20:254–60.
20. Hao Y, Li D, Xu Y, Ouyang J, Wang Y, Zhang Y, Li B, Xie L, Qin G. Investigation of lipid metabolism dysregulation and the effects on immune microenvironments in pan-cancer using multiple omics data. BMC Bioinformatics. 2019;20:195.
21. Lu L, Li ZJ, Li LF, Wu WK, Shen J, Zhang L, Chan RL, Yu L, Liu YW, Ren SX, Chan KM, Cho CH. Vascular-targeted TNFalpha improves tumor blood vessel function and enhances antitumor immunity and chemotherapy in colorectal cancer. J Control Release. 2015;210:134–46.
22. Fearon KC, Glass DJ, Guttridge DC. Cancer cachexia: mediators, signaling, and metabolic pathways. Cell Metab. 2012;16:153–66.
23. Rodriguez-Broadbent H, Law PJ, Sud A, Palin K, Tuupanen S, Gylfe A, Hänninen UA, Cajuso T, Tanskanen T, Kondelin J, Kaasinen E, Sarin AP, Ripatti S, Eriksson JG, Rissanen H, Knekt P, Pukkala E, Jousilahti P, Salomaa V, Palotie A, Renkonen-Sinisalo L, Lepistö A, Böhm J, Mecklin JP, Al-Tassan NA, Palles C, Martin L, Barclay E, Farrington SM, Timofeeva MN, Meyer BF, Wakil SM, Campbell H, Smith CG, Idziaszczyk S, Maughan TS, Kaplan R, Kerr R, Kerr D, Passarelli MN, Figueiredo JC, Buchanan DD, Win AK, Hopper JL, Jenkins MA, Lindor NM, Newcomb PA, Gallinger S, Conti D, Schumacher F, Casey G, Aaltonen LA, Cheadle JP, Tomlinson IP, Dunlop MG, Houlston RS. Mendelian randomisation implicates hyperlipidaemia as a risk factor for colorectal cancer. Int J Cancer. 2017;140:2701–8.

Figures

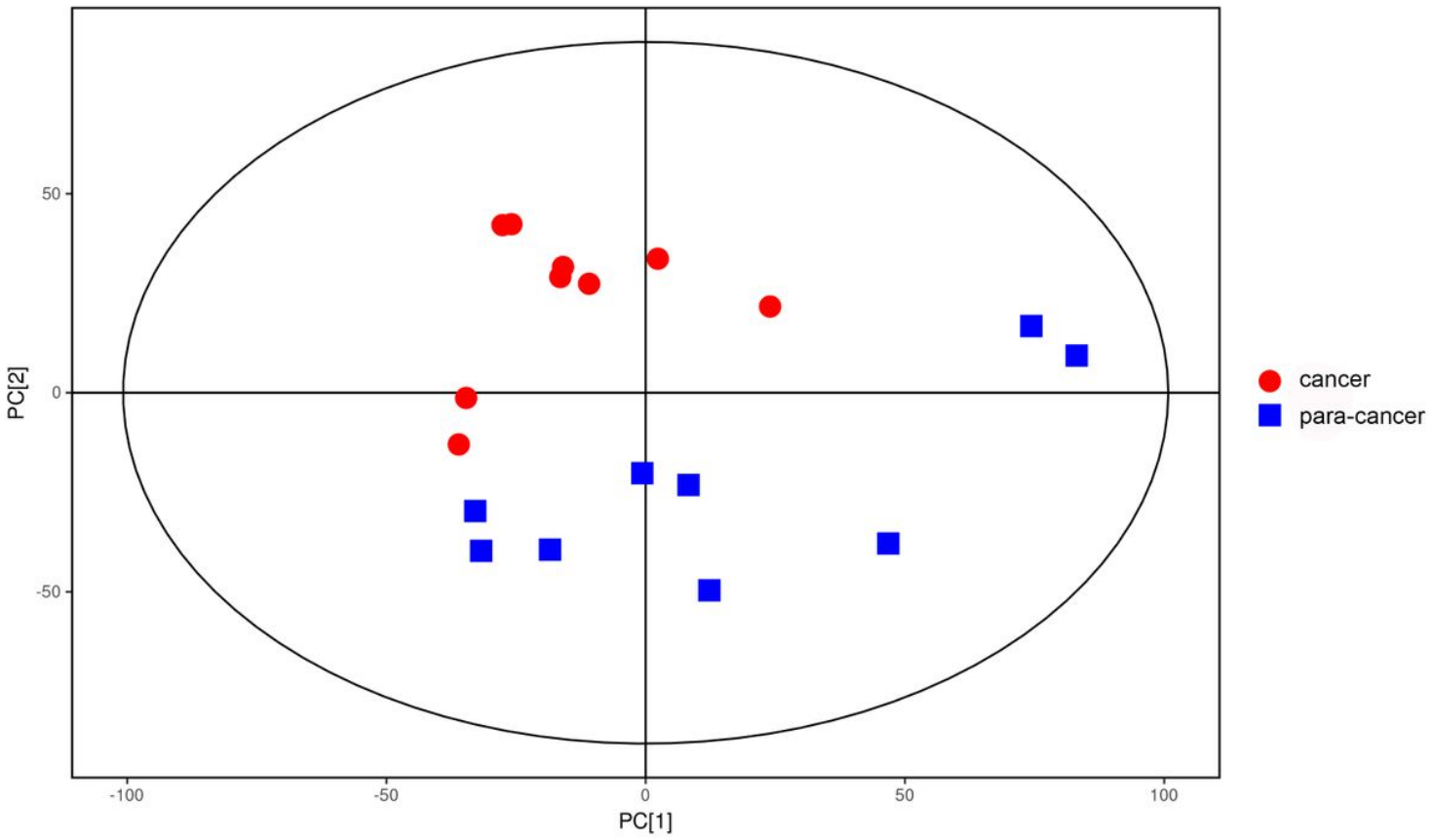

Figure 1

Score scatter plot of PCA model for cancer group versus para-carcinoma tissue group.

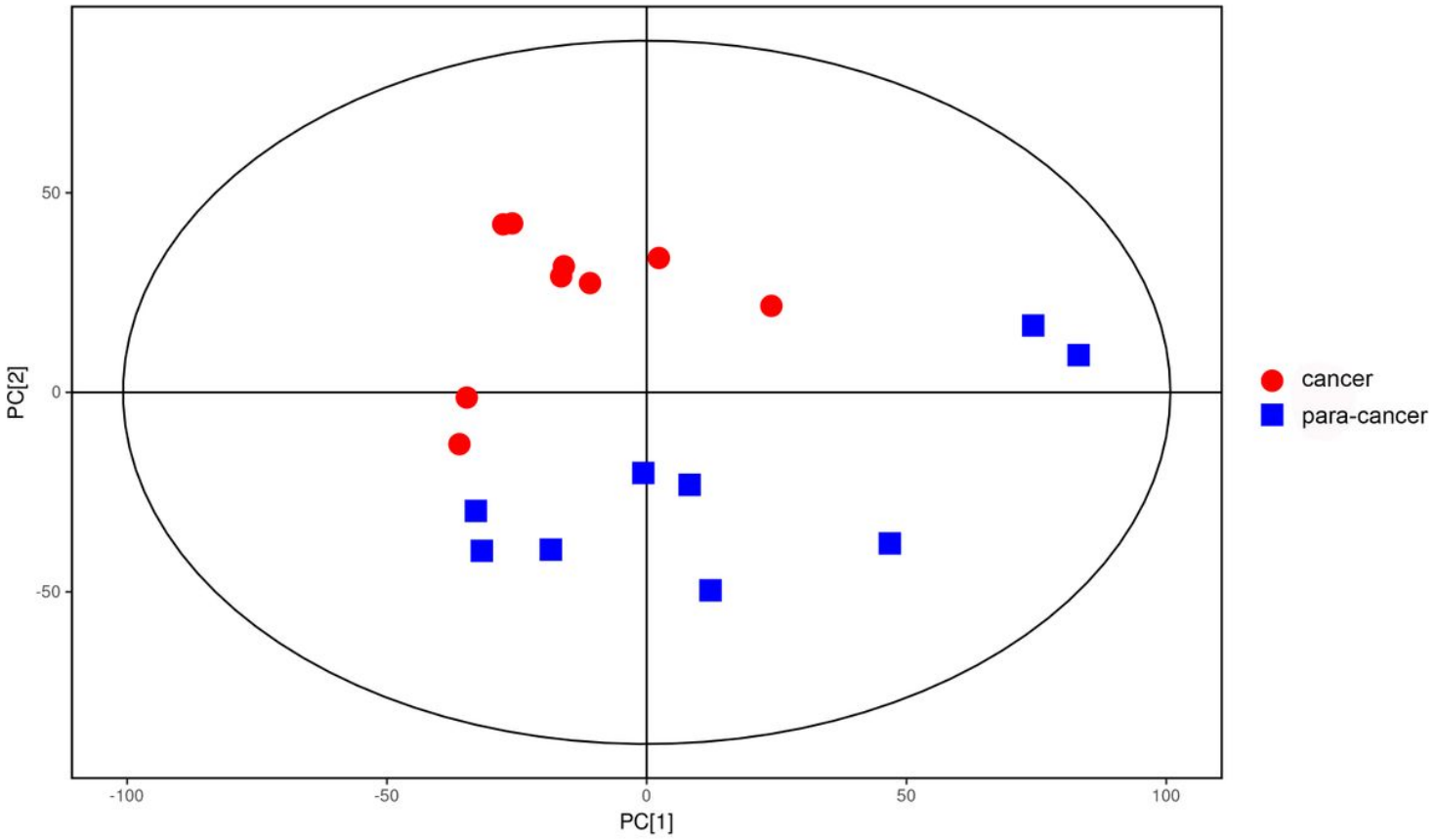

Figure 1

Score scatter plot of PCA model for cancer group versus para-carcinoma tissue group.

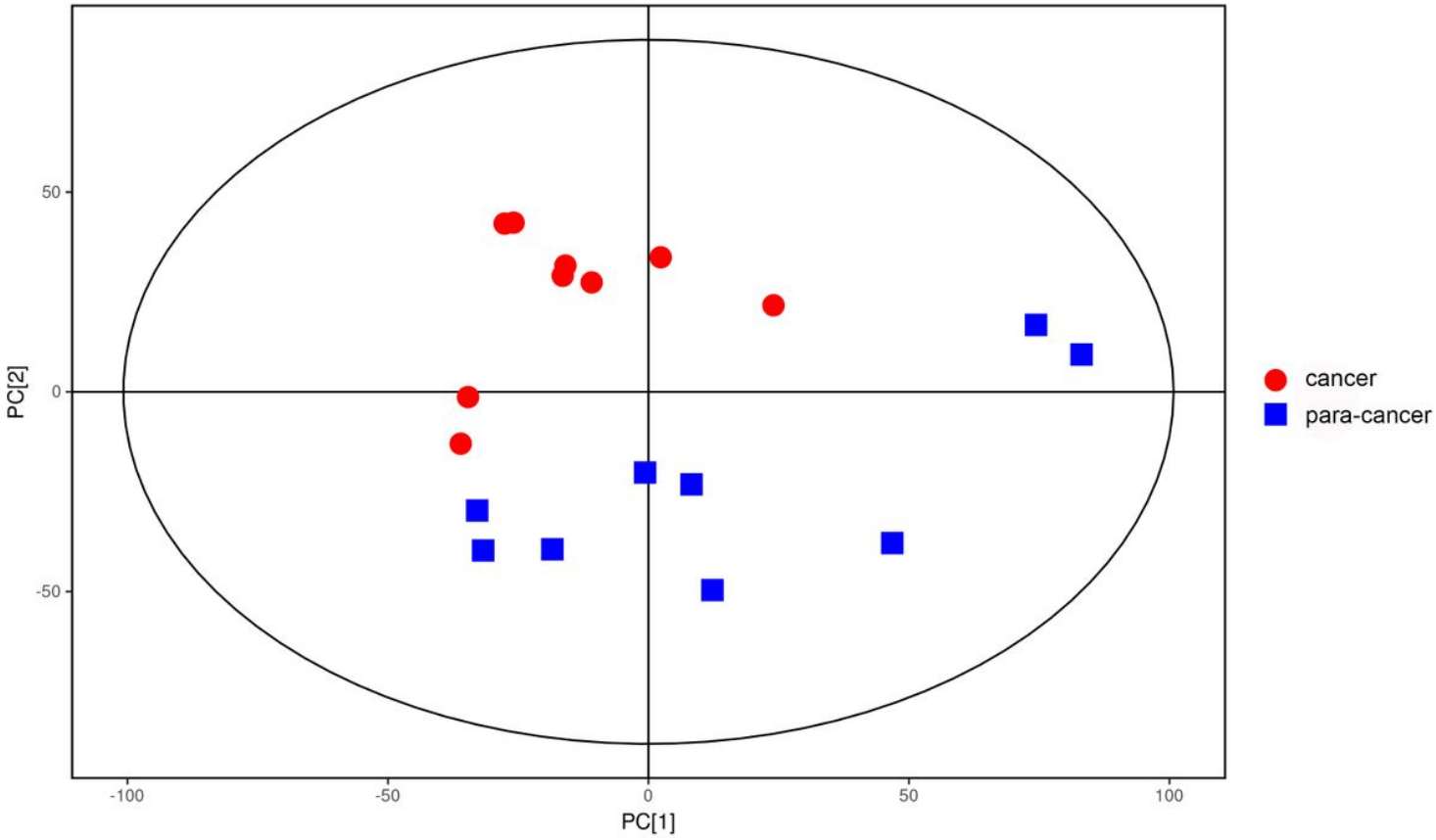

Figure 1

Score scatter plot of PCA model for cancer group versus para-carcinoma tissue group.

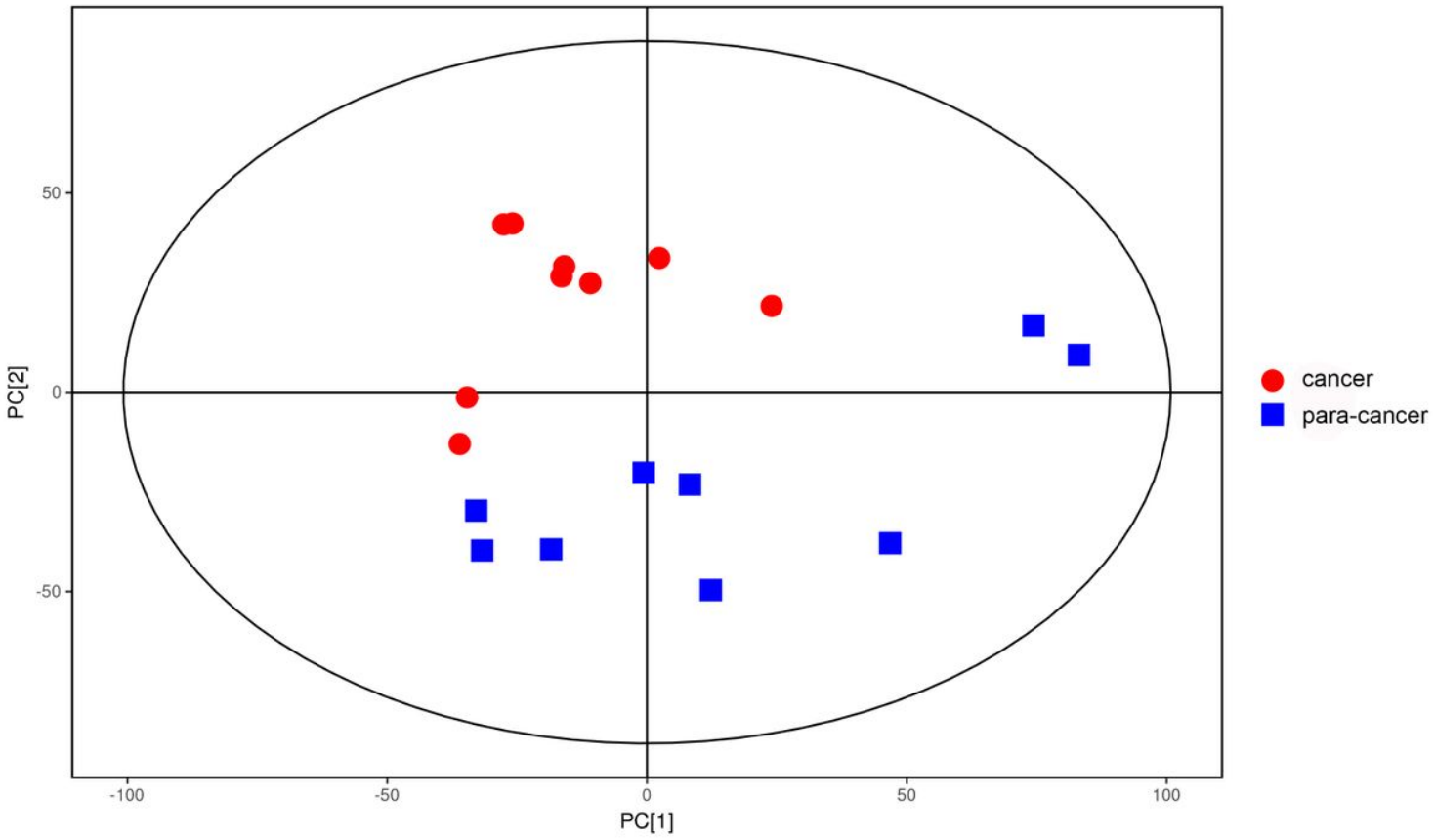

Figure 1

Score scatter plot of PCA model for cancer group versus para-carcinoma tissue group.

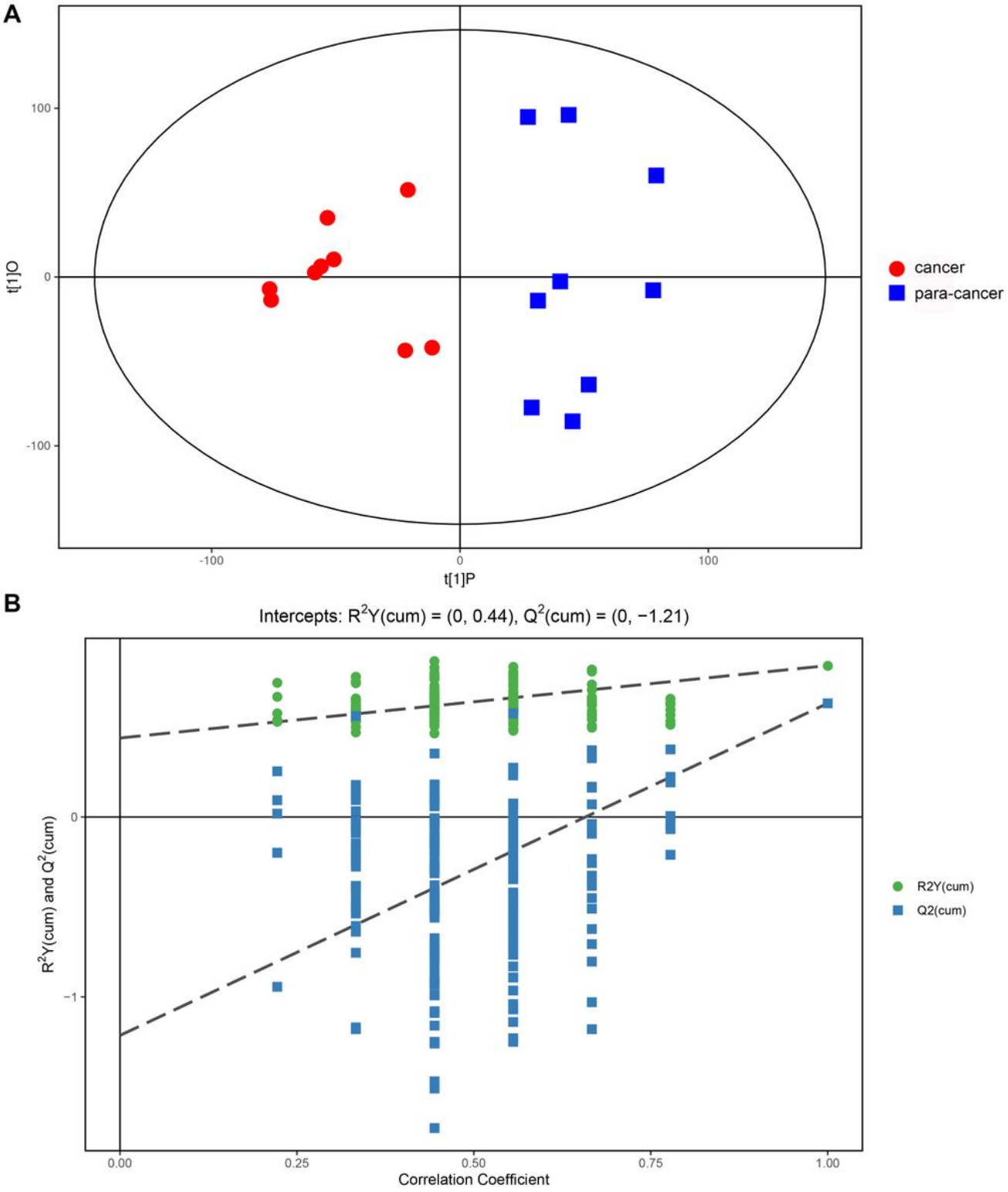

Figure 2

(A) Score scatter plot of OPLS-DA model for the cancer group versus the para-cancer group. (B) Permutation test of OPLS-DA model for the cancer group versus the para-cancer group.

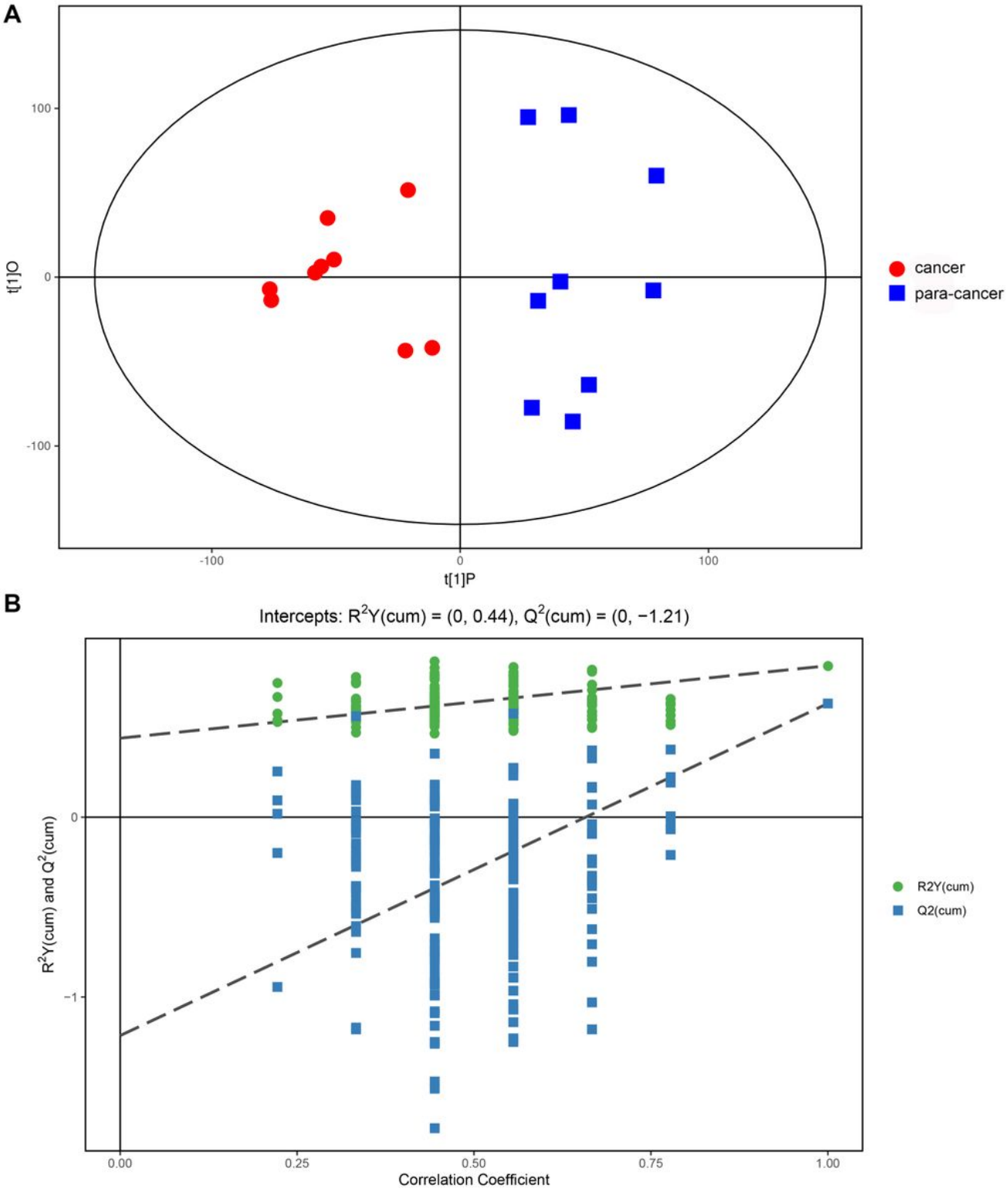

Figure 2

(A) Score scatter plot of OPLS-DA model for the cancer group versus the para-cancer group. (B) Permutation test of OPLS-DA model for the cancer group versus the para-cancer group.

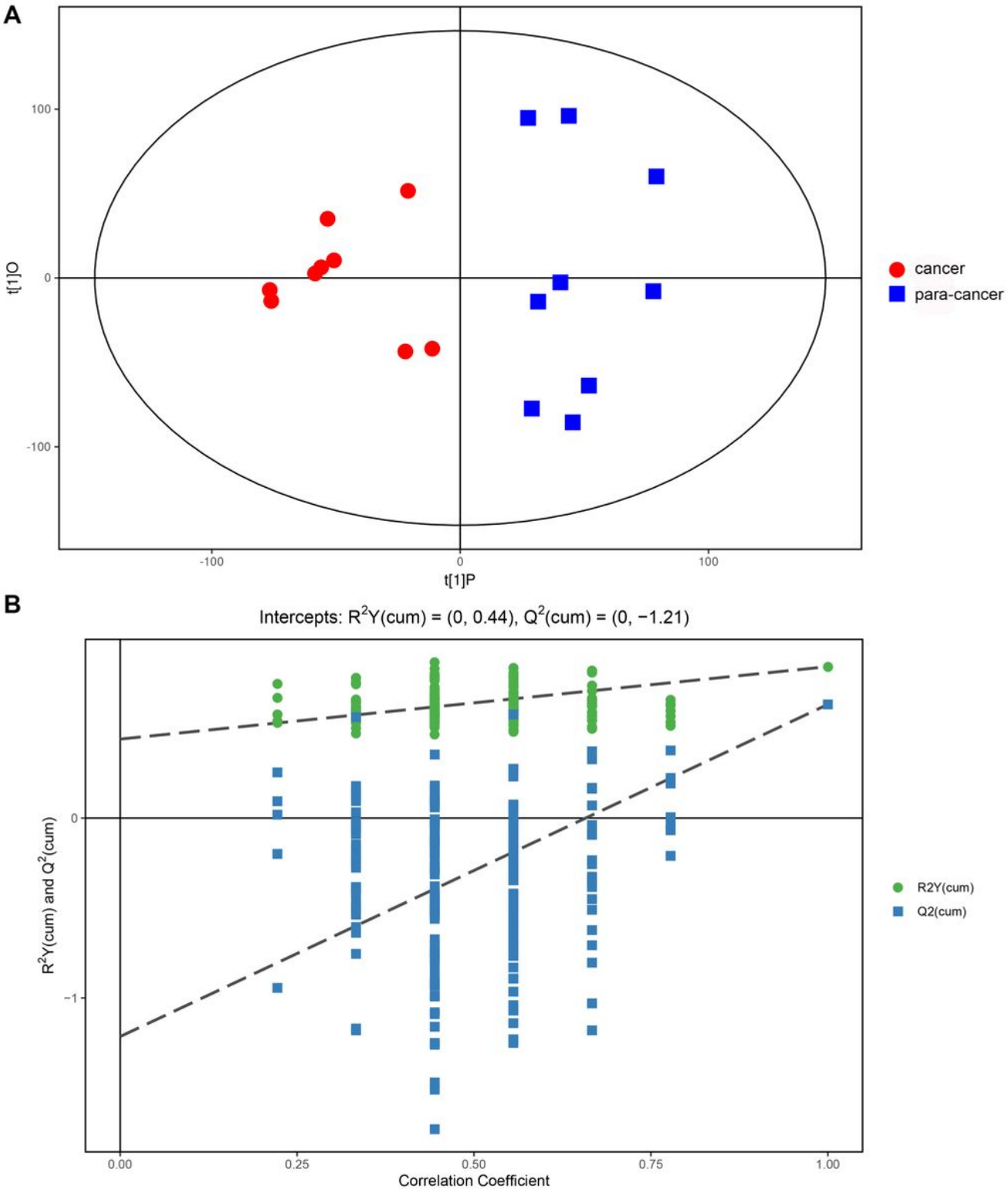

Figure 2

(A) Score scatter plot of OPLS-DA model for the cancer group versus the para-cancer group. (B) Permutation test of OPLS-DA model for the cancer group versus the para-cancer group.

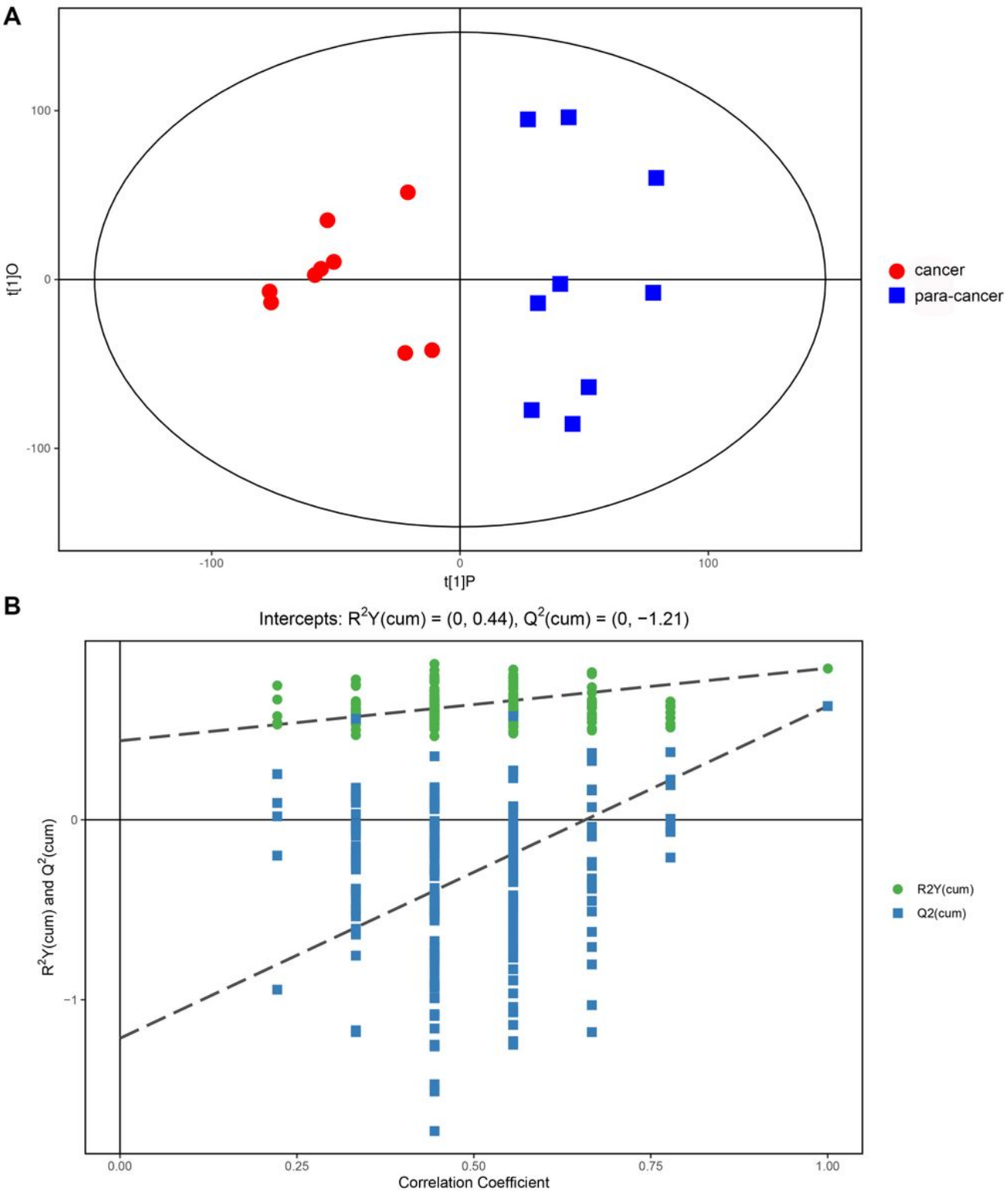

Figure 2

(A) Score scatter plot of OPLS-DA model for the cancer group versus the para-cancer group. (B) Permutation test of OPLS-DA model for the cancer group versus the para-cancer group.

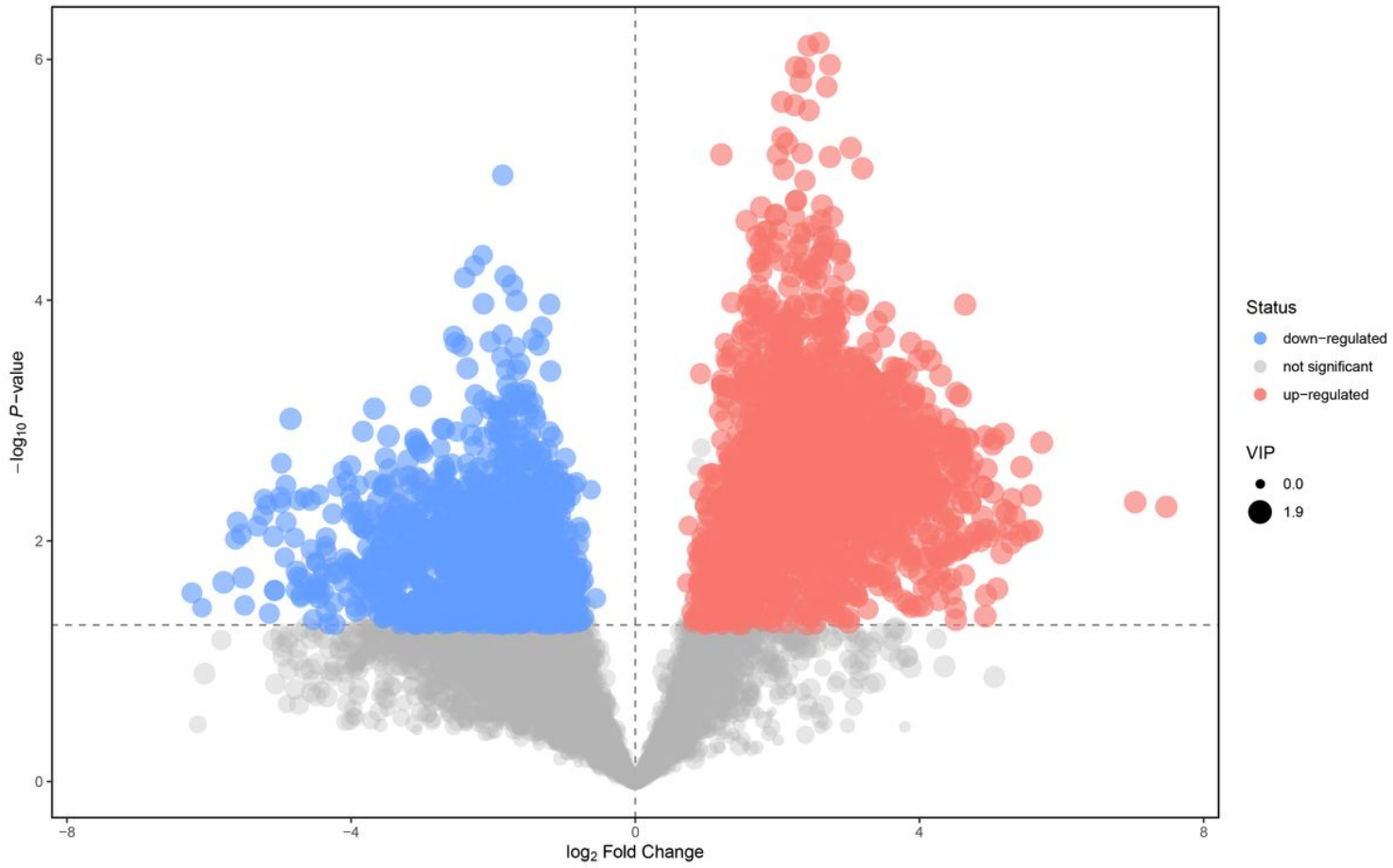

Figure 3

Volcano plot for the cancer group versus the para-cancer group.

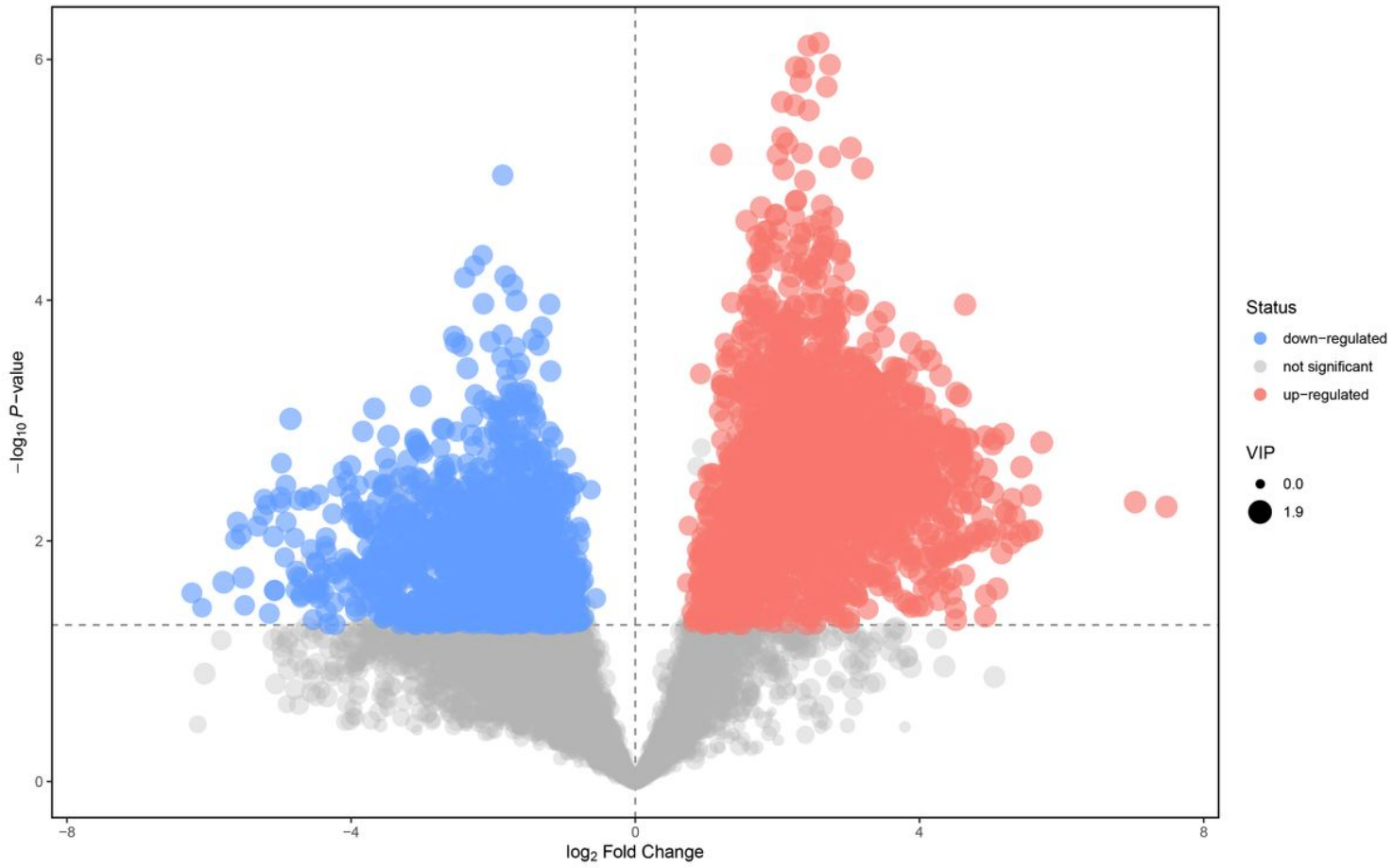

Figure 3

Volcano plot for the cancer group versus the para-cancer group.

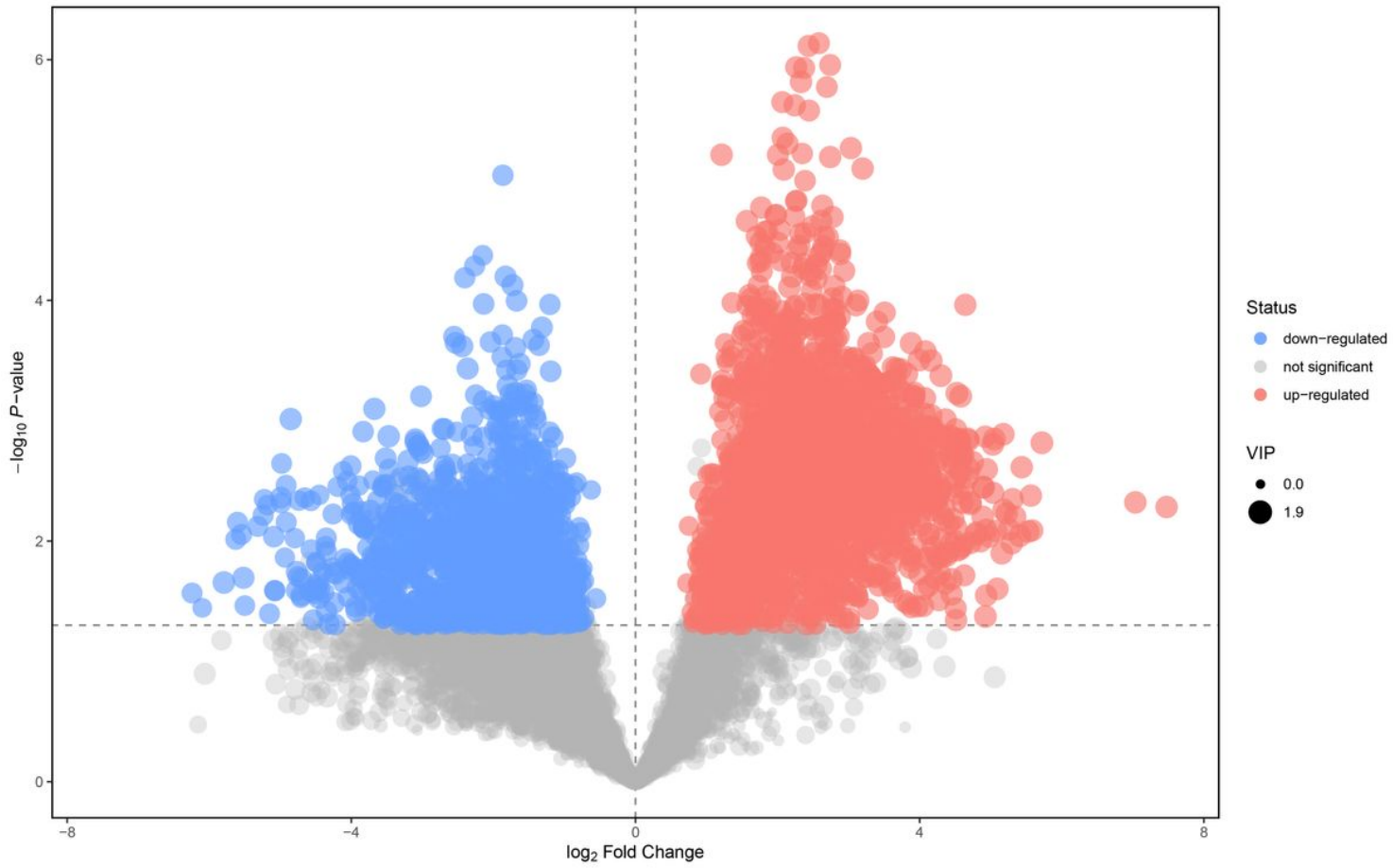

Figure 3

Volcano plot for the cancer group versus the para-cancer group.

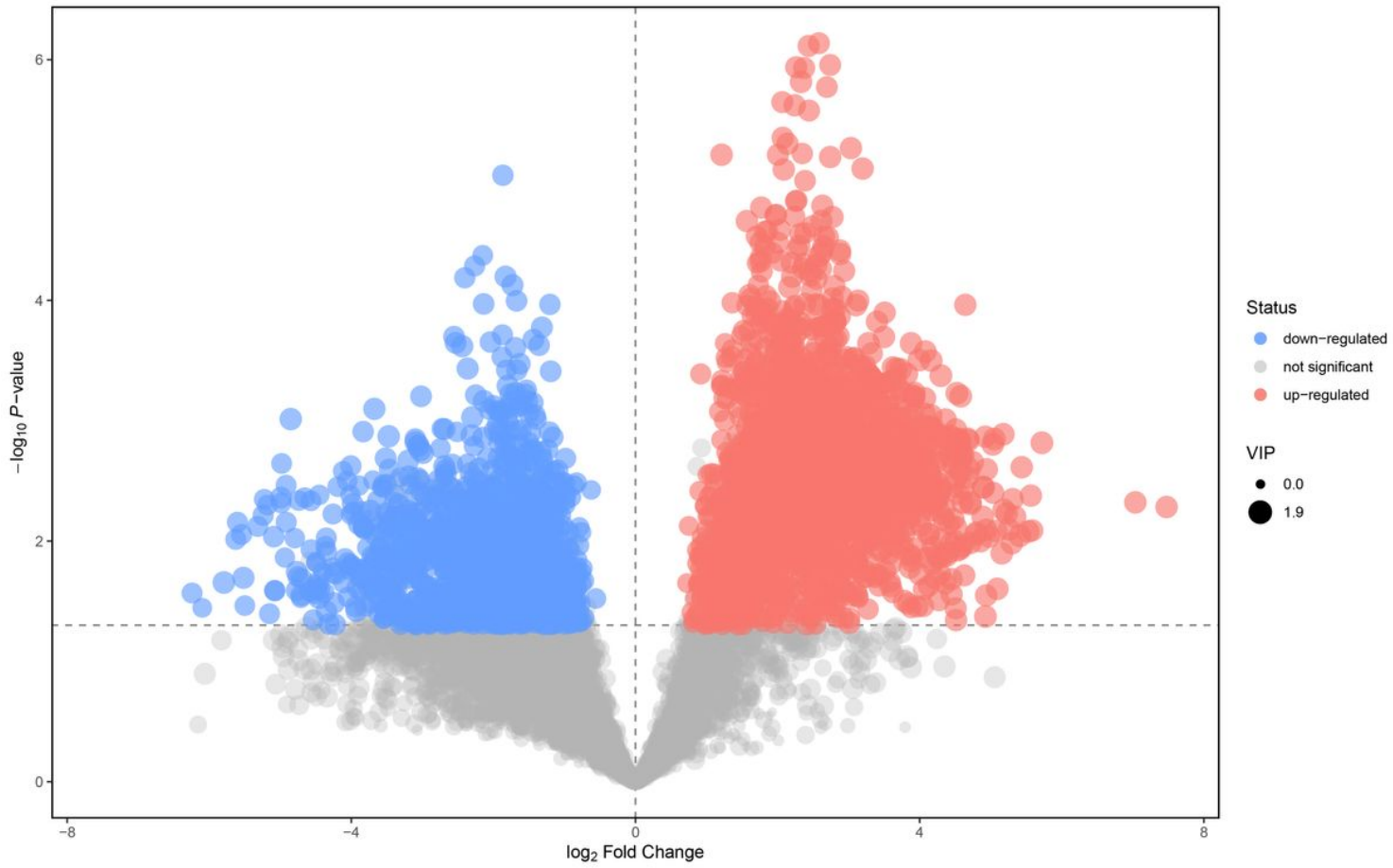

Figure 3

Volcano plot for the cancer group versus the para-cancer group.

Figure 4

Heat map of hierarchical clustering analysis for the cancer group versus the para-cancer group.

Figure 4

Heat map of hierarchical clustering analysis for the cancer group versus the para-cancer group.

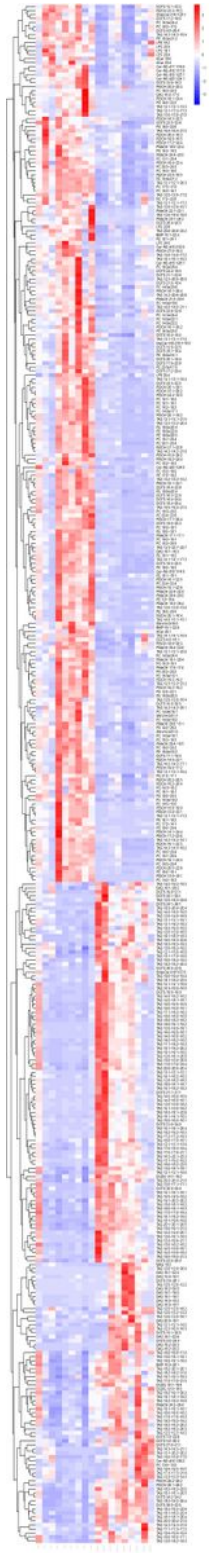

Figure 4

Heat map of hierarchical clustering analysis for the cancer group versus the para-cancer group.

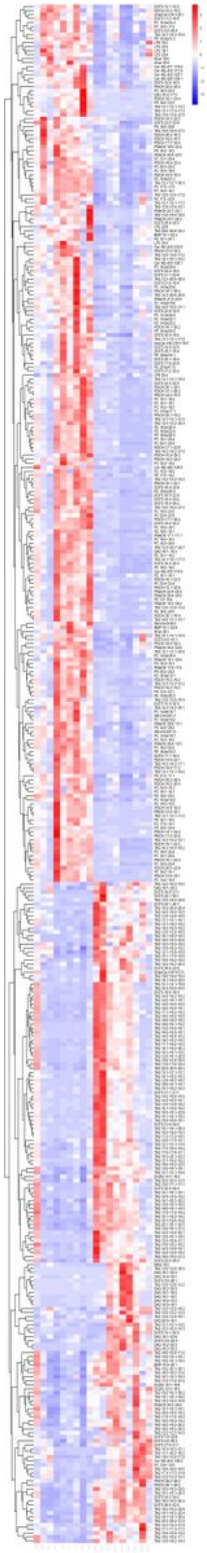

Figure 4

Heat map of hierarchical clustering analysis for the cancer group versus the para-cancer group.

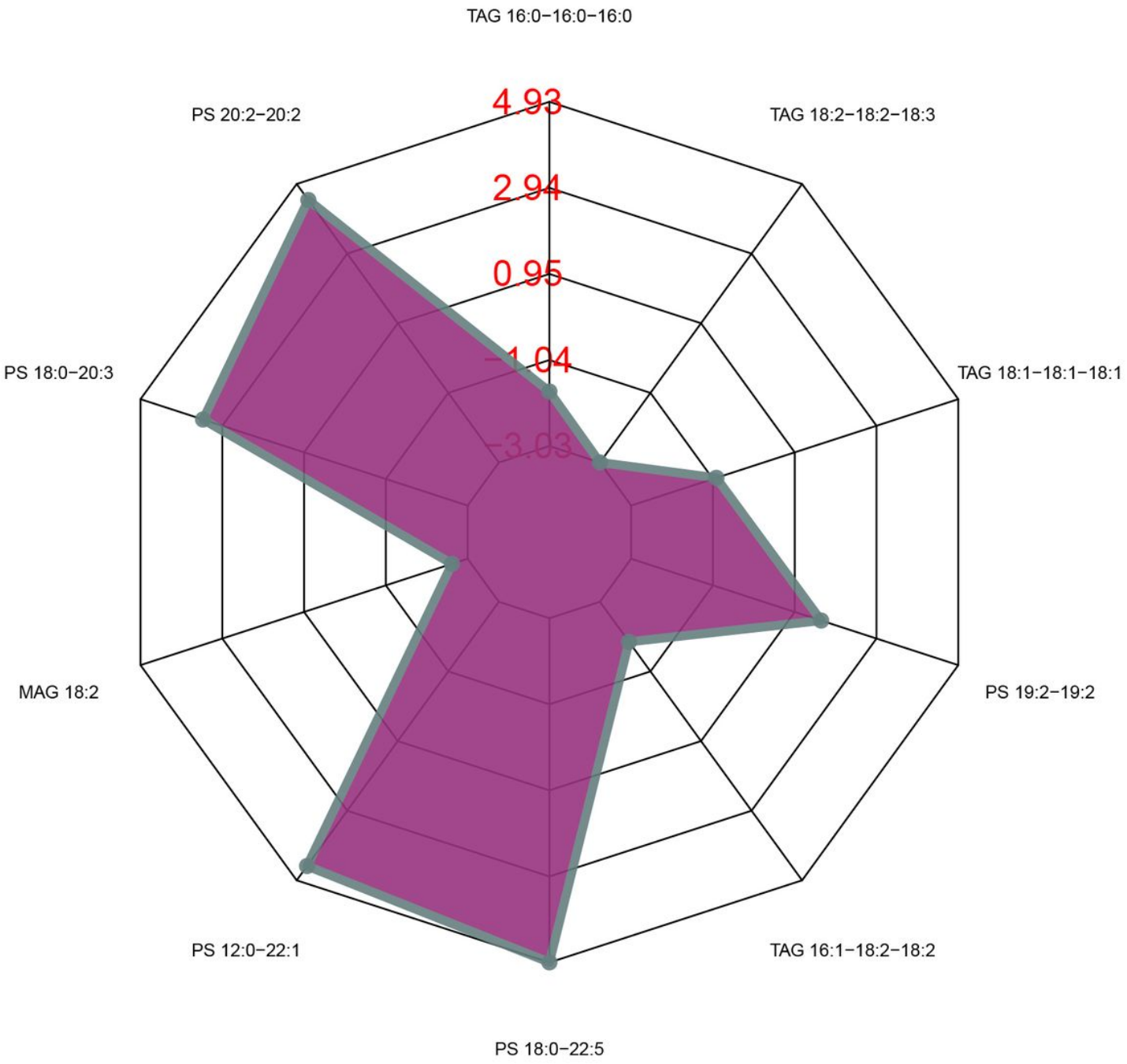

Figure 5

Radar chart analysis for the cancer group versus the para-cancer group.

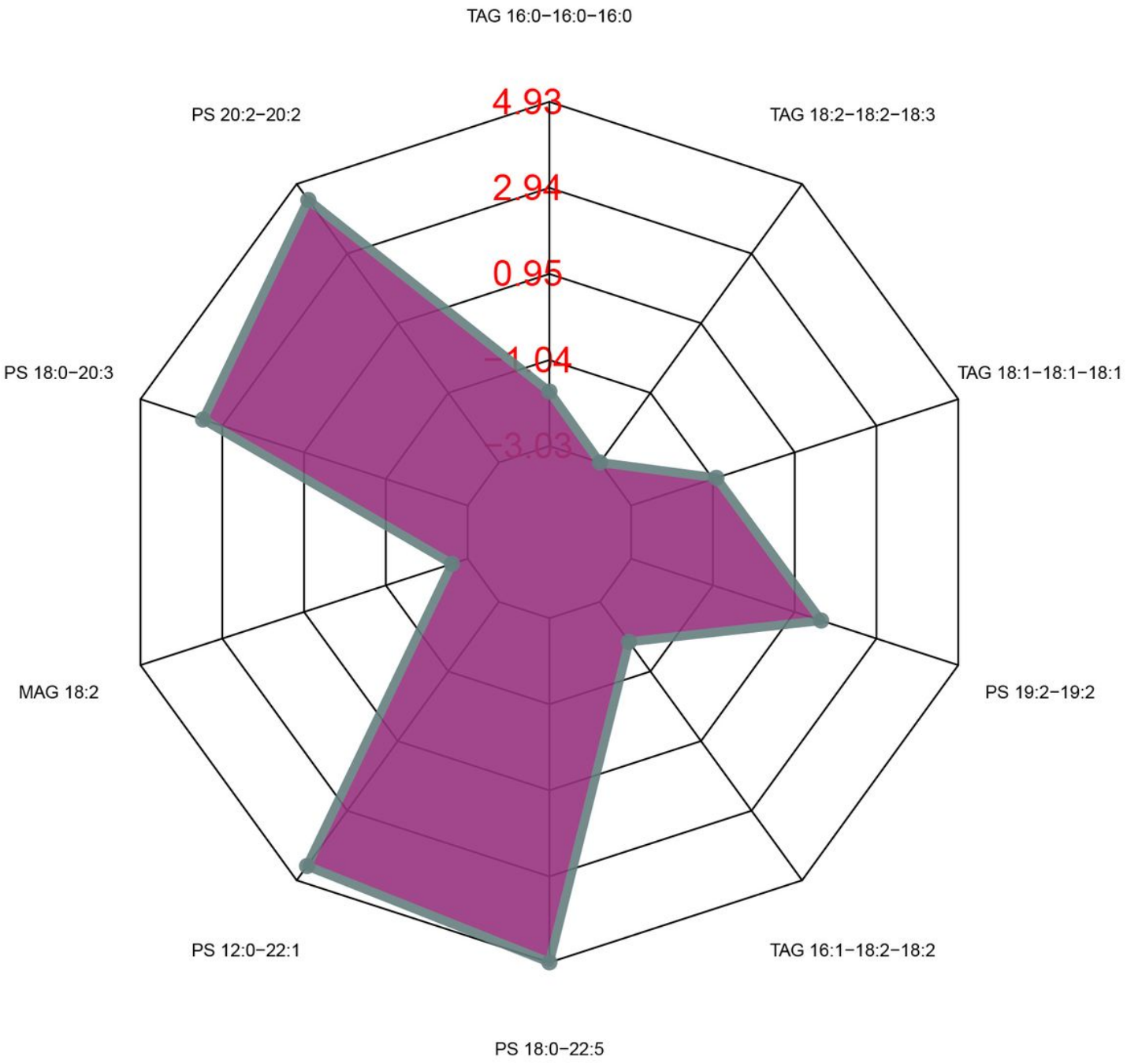

Figure 5

Radar chart analysis for the cancer group versus the para-cancer group.

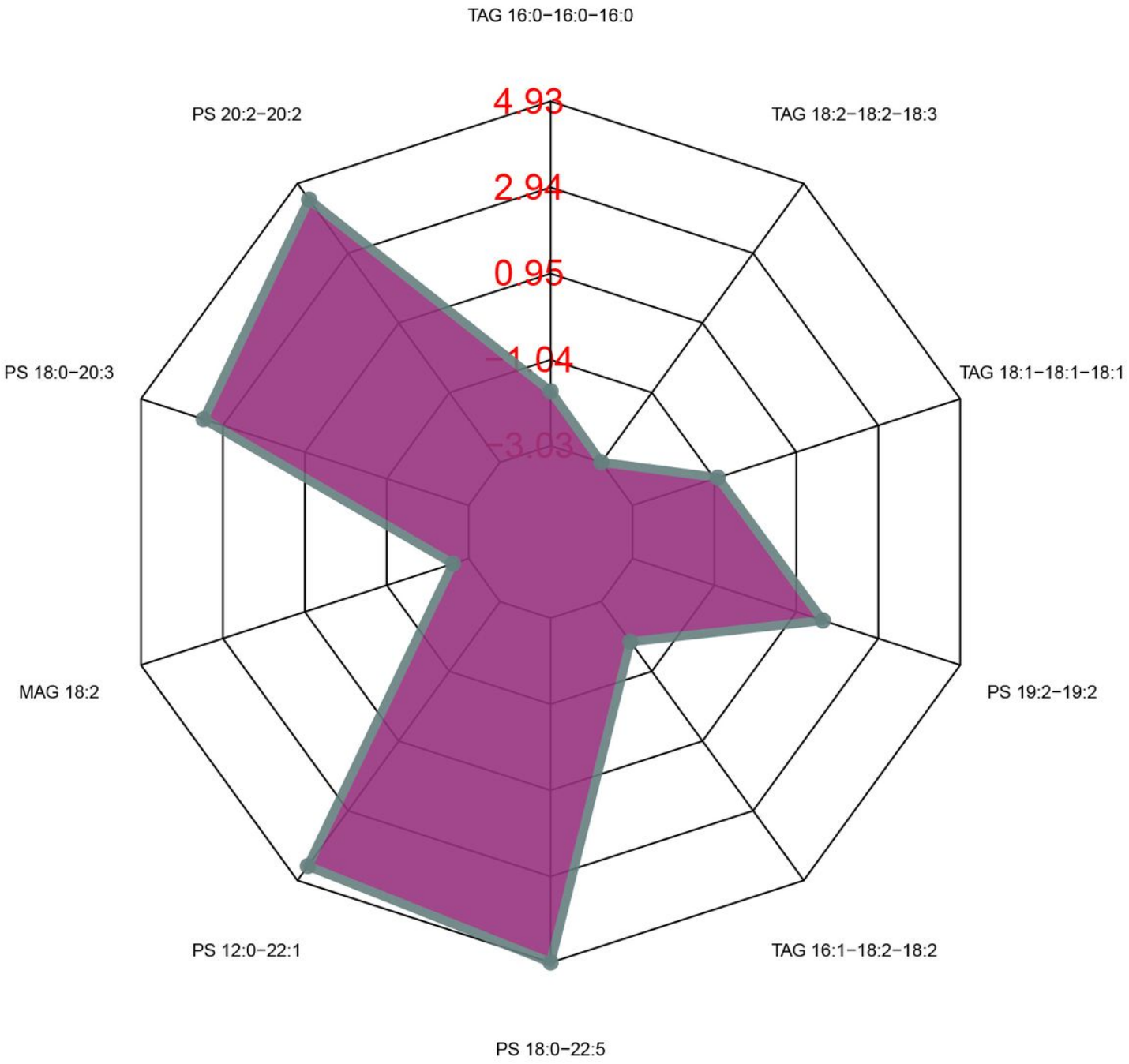

Figure 5

Radar chart analysis for the cancer group versus the para-cancer group.

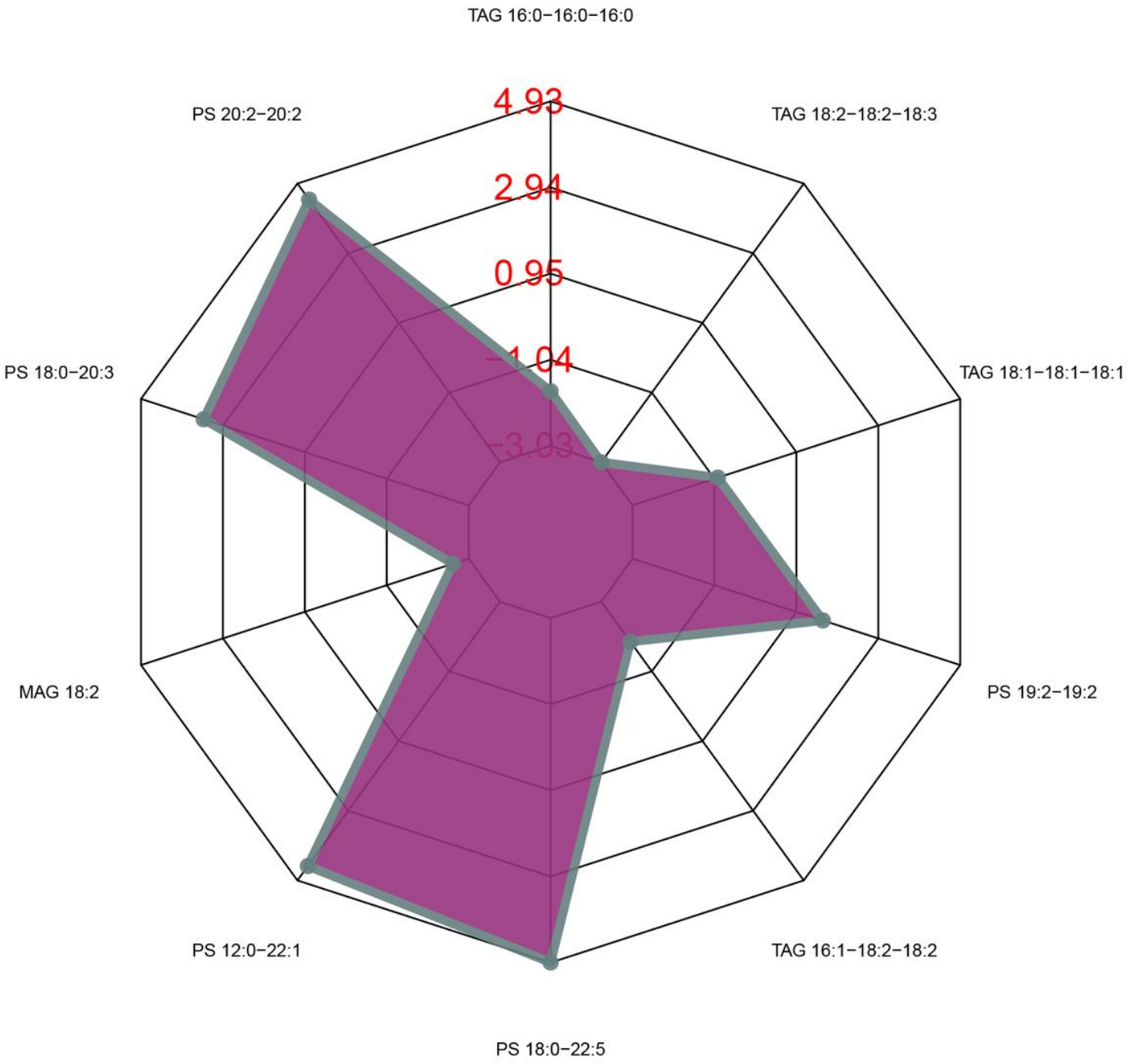

Figure 5

Radar chart analysis for the cancer group versus the para-cancer group.

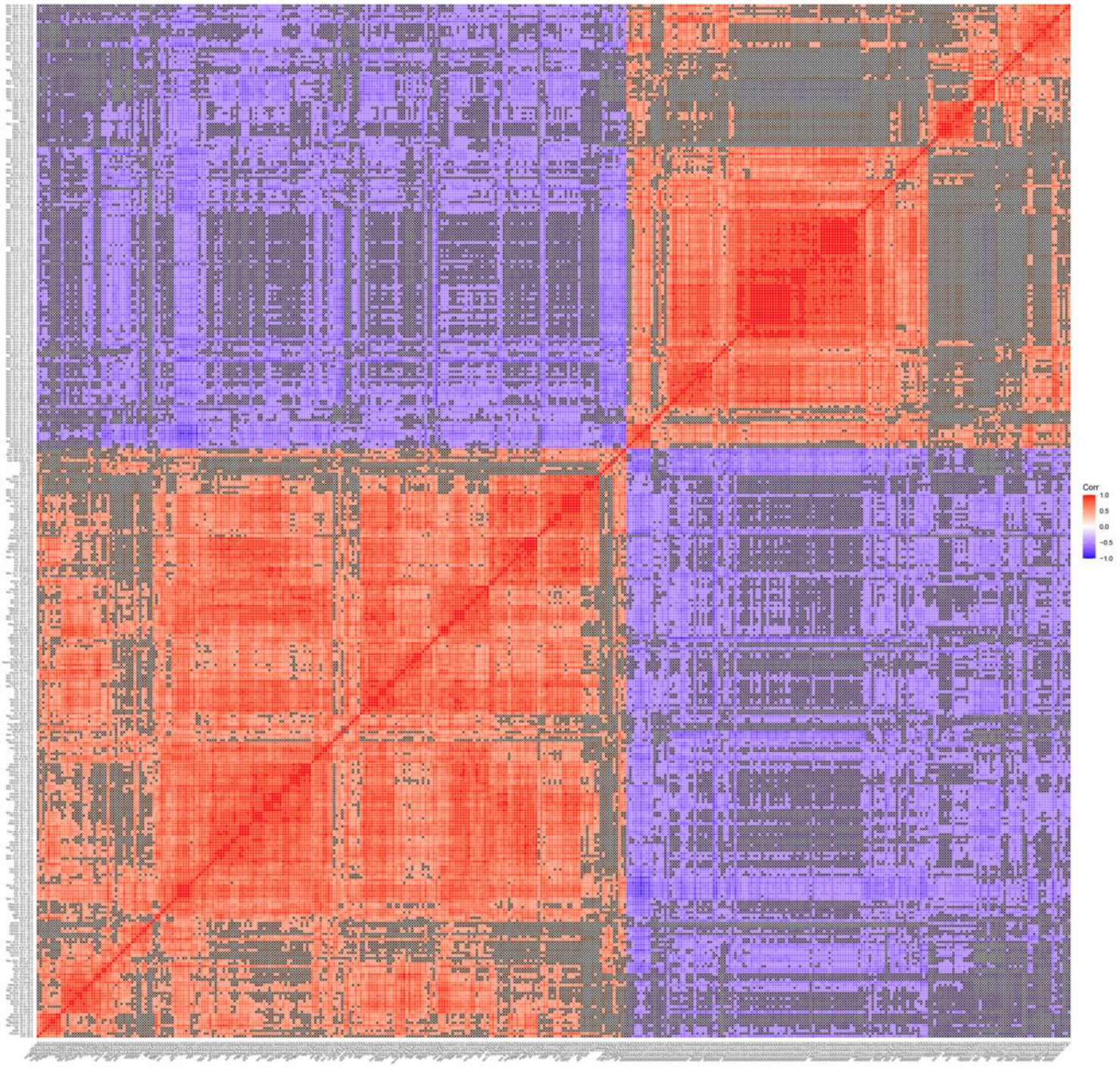

Figure 6

Heatmap of correlation analysis for the cancer group versus the para-cancer group.

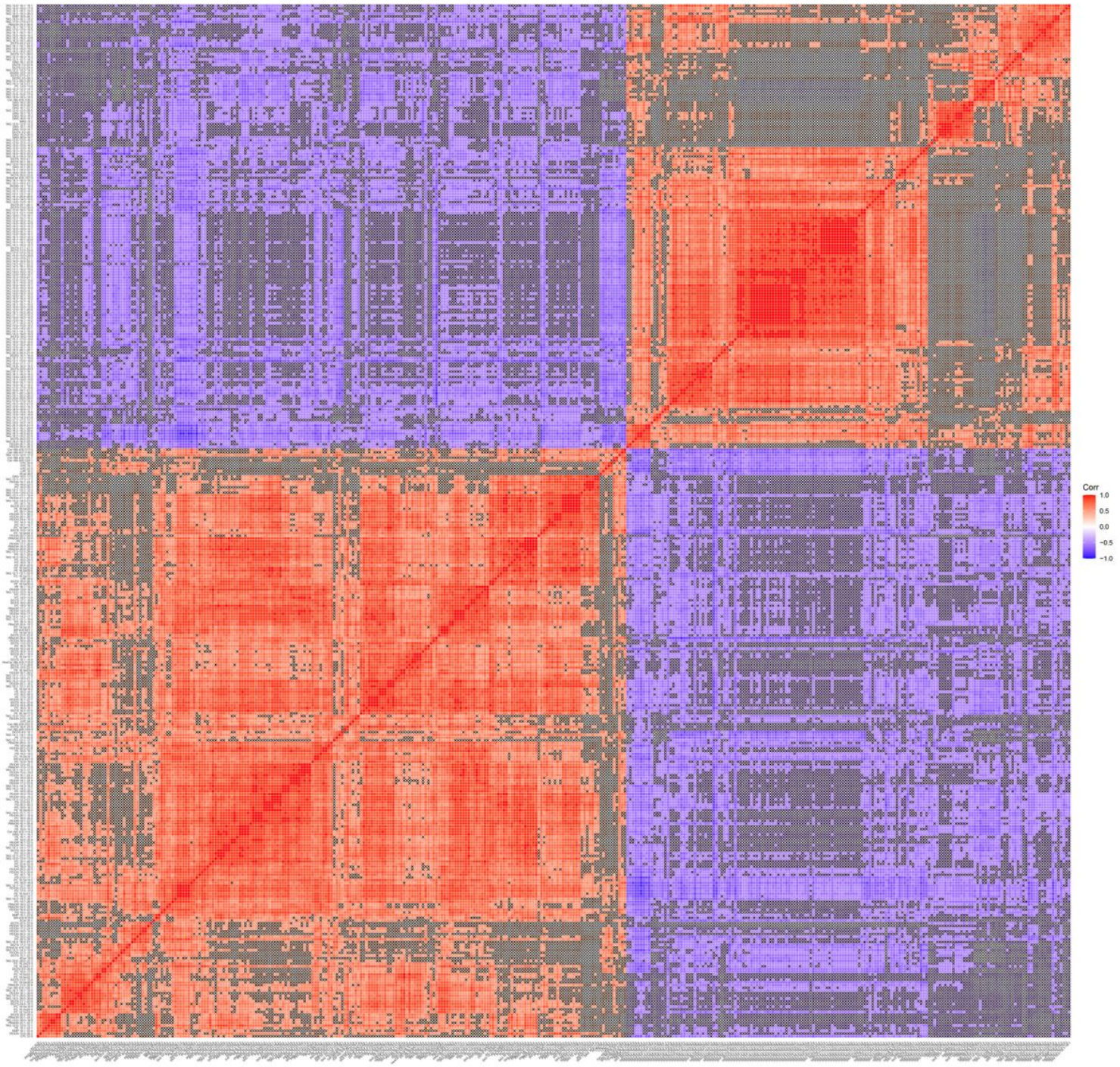

Figure 6

Heatmap of correlation analysis for the cancer group versus the para-cancer group.

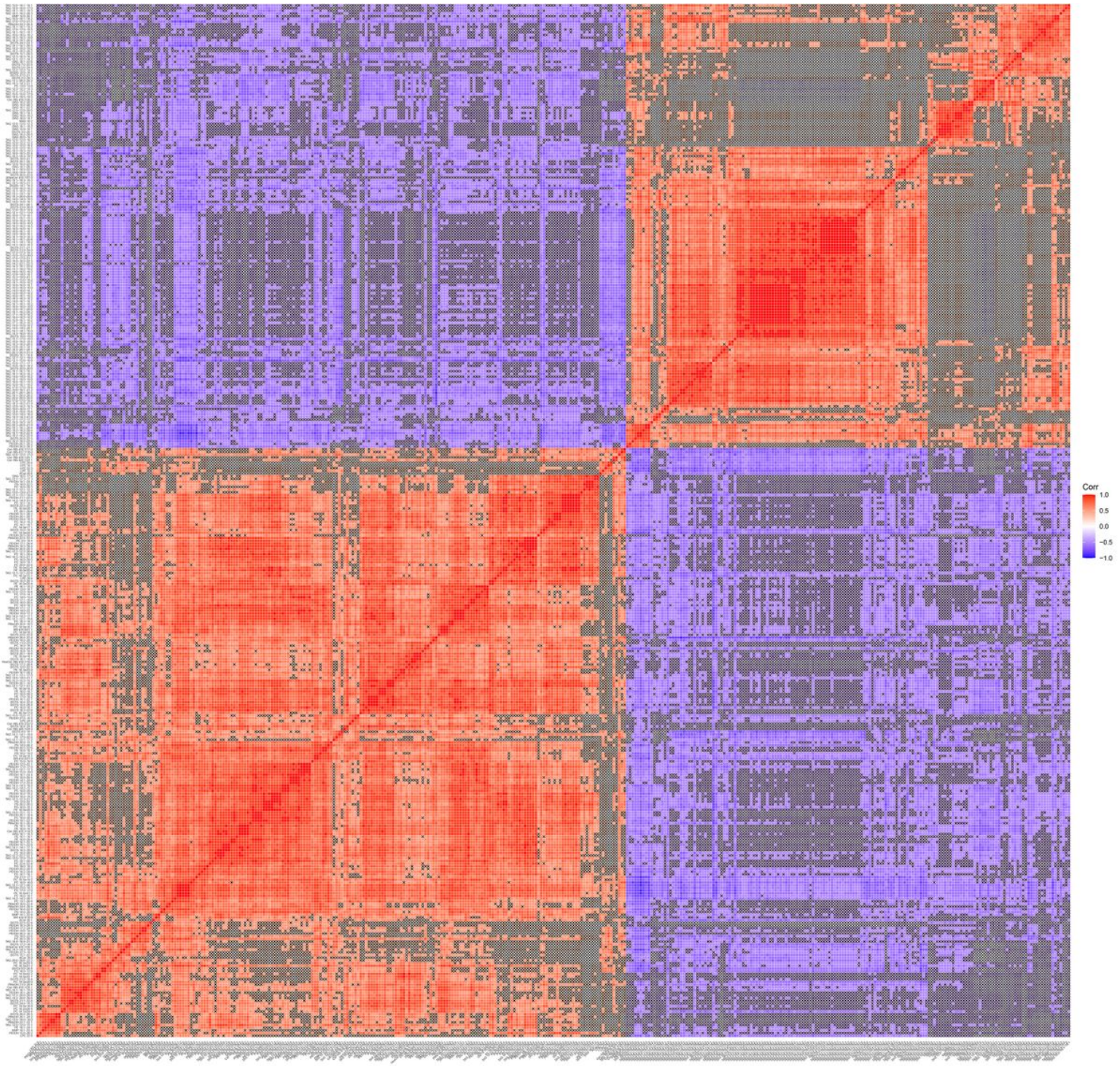

Figure 6

Heatmap of correlation analysis for the cancer group versus the para-cancer group.

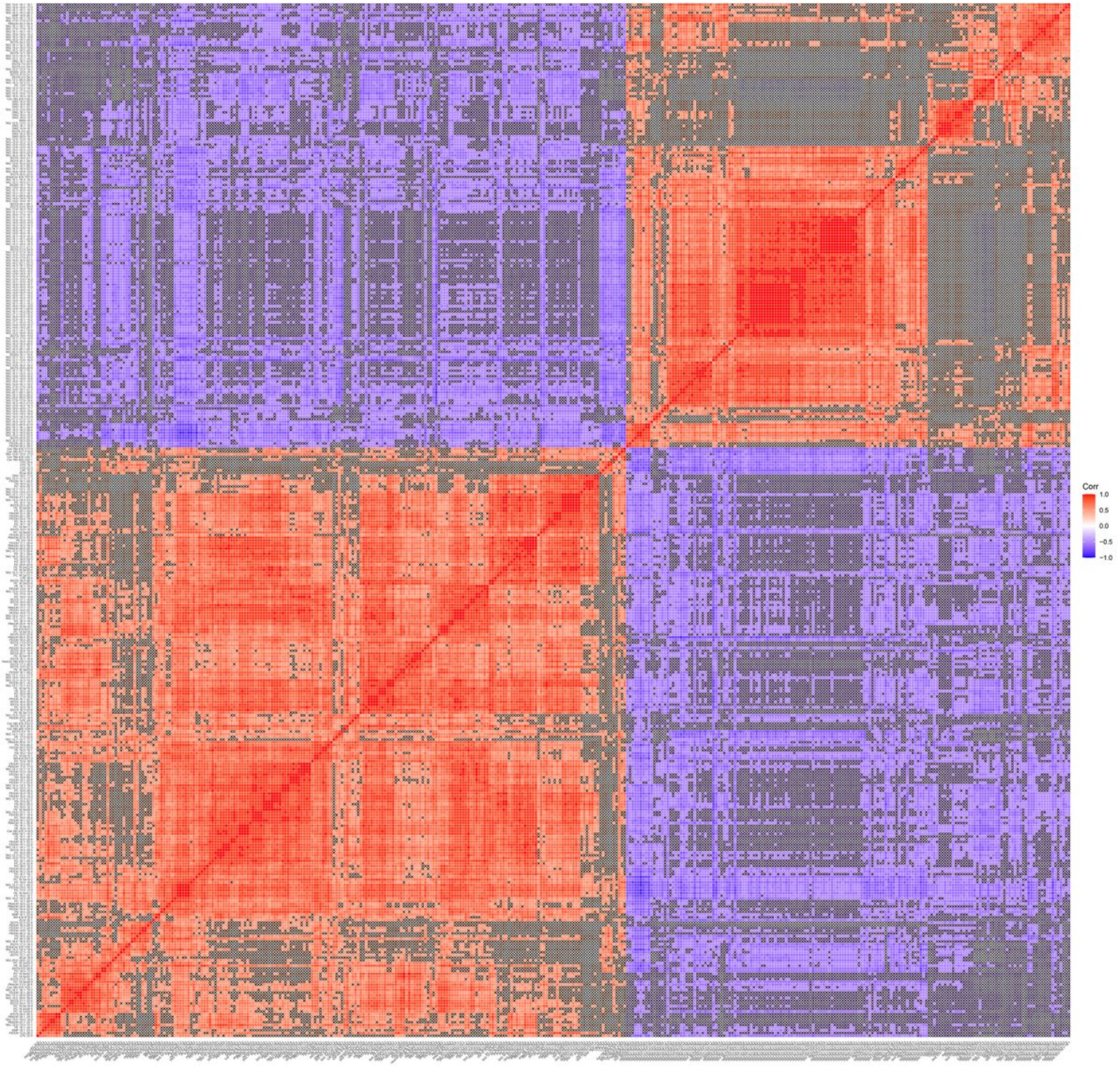

Figure 6

Heatmap of correlation analysis for the cancer group versus the para-cancer group.

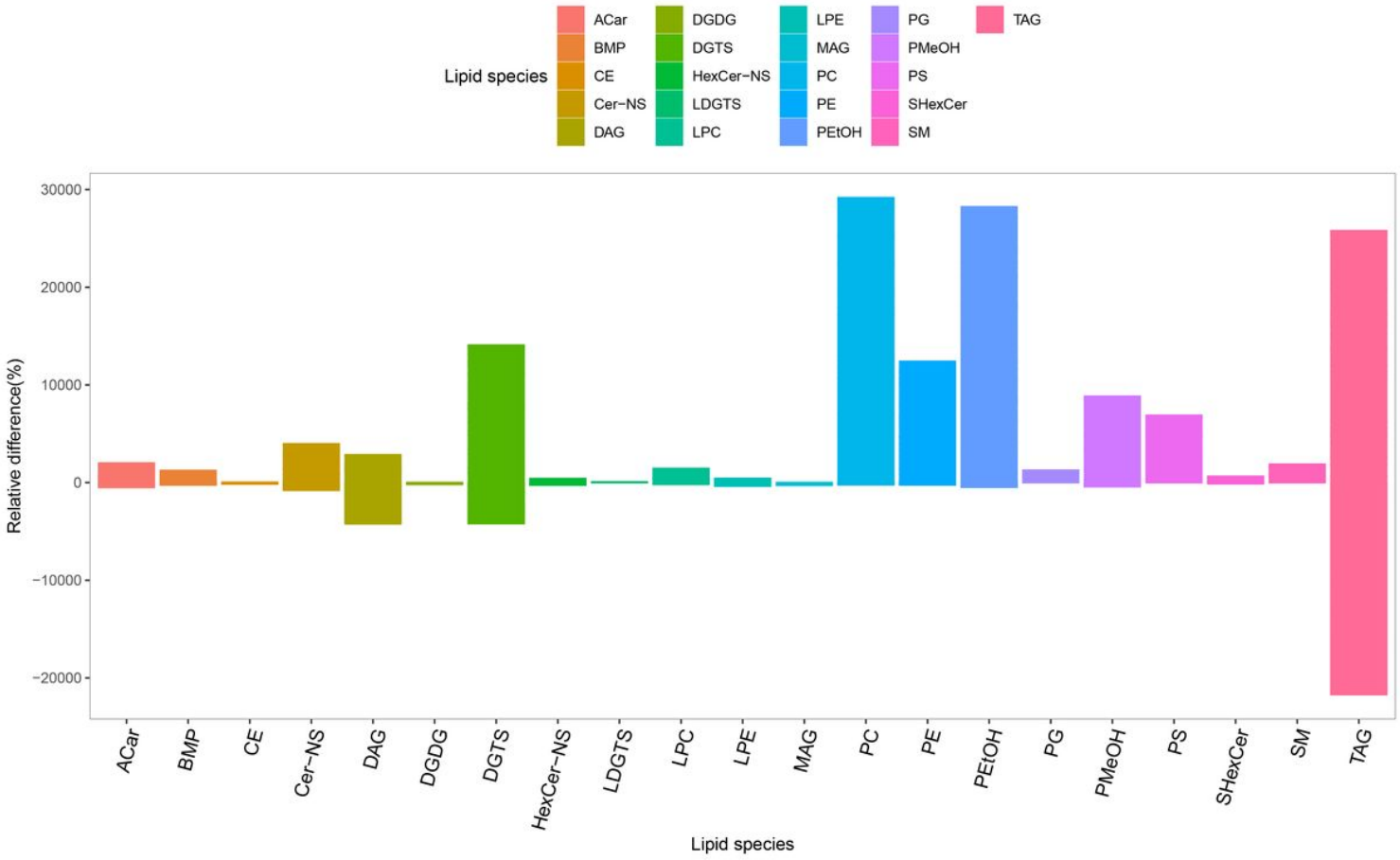

Figure 7

Bar plot for the cancer group versus the para-cancer group.

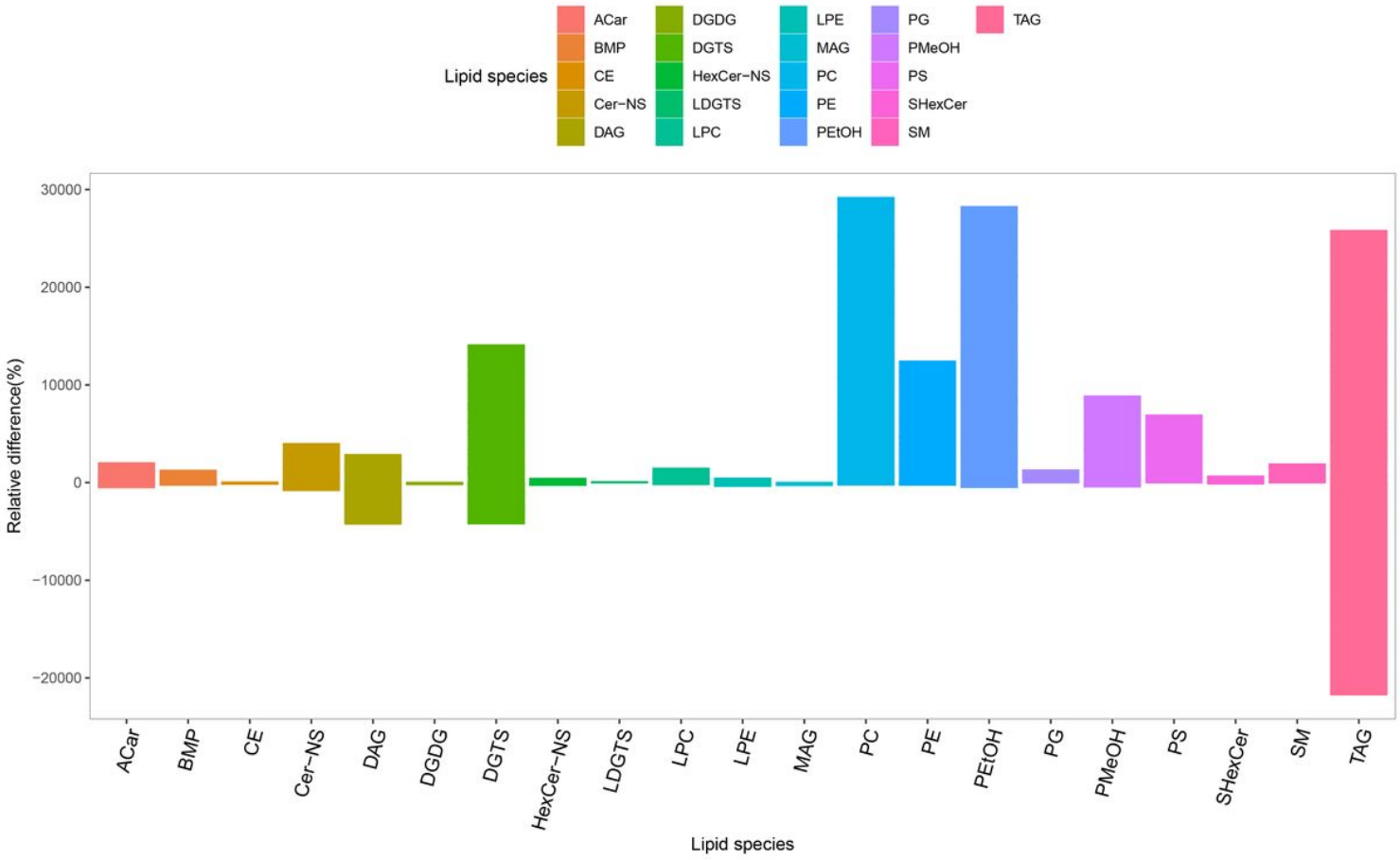

Figure 7

Bar plot for the cancer group versus the para-cancer group.

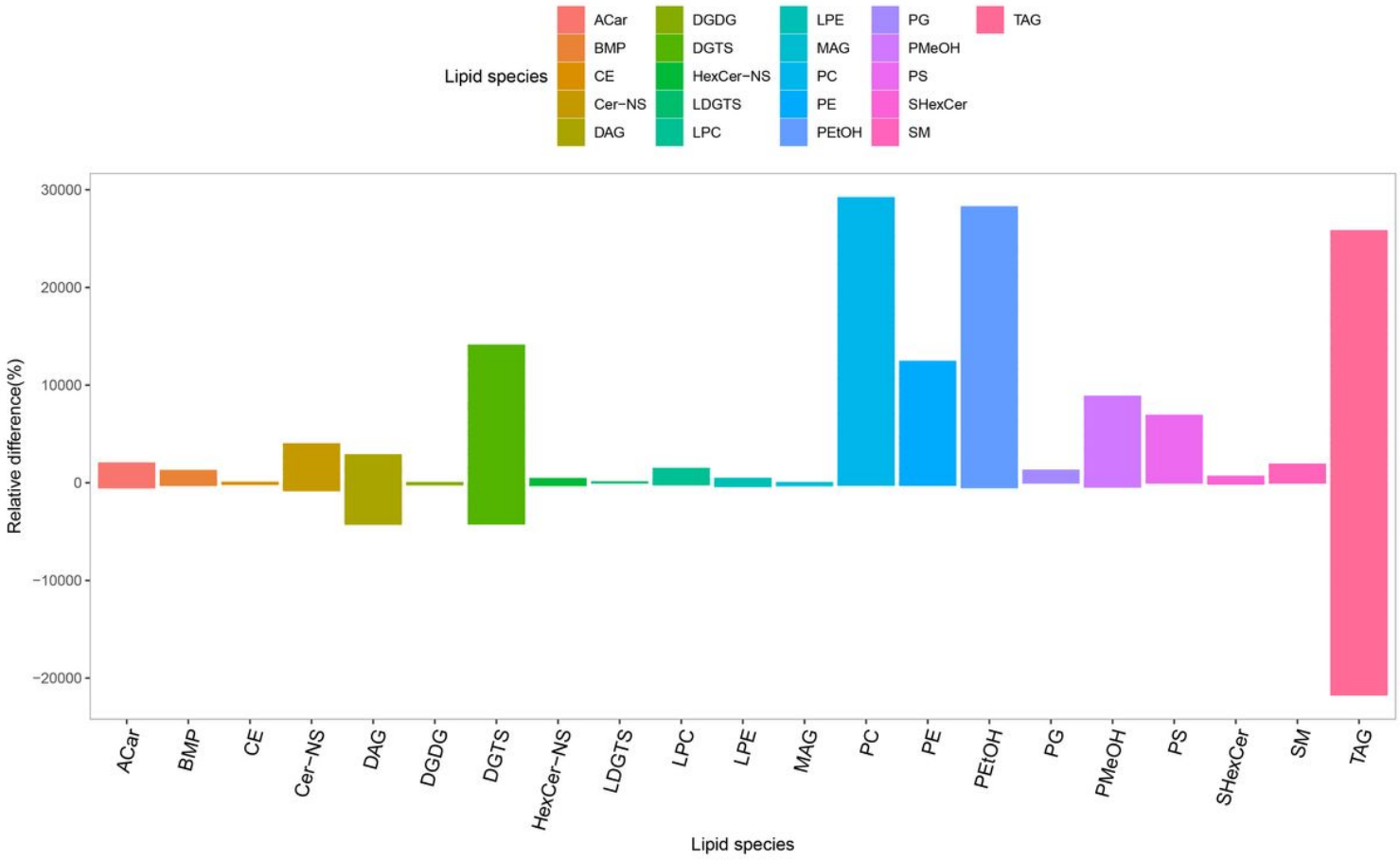

Figure 7

Bar plot for the cancer group versus the para-cancer group.

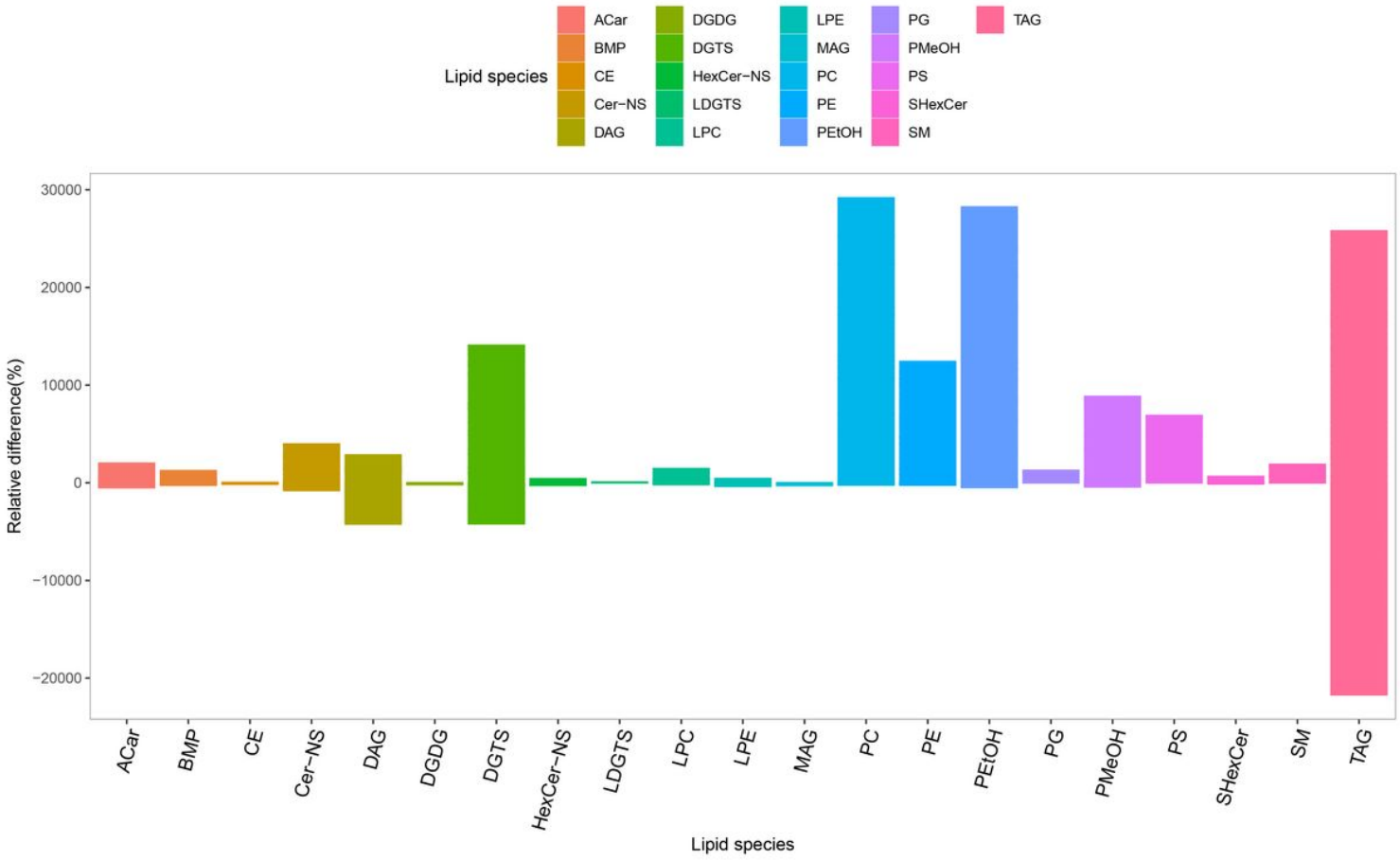

Figure 7

Bar plot for the cancer group versus the para-cancer group.

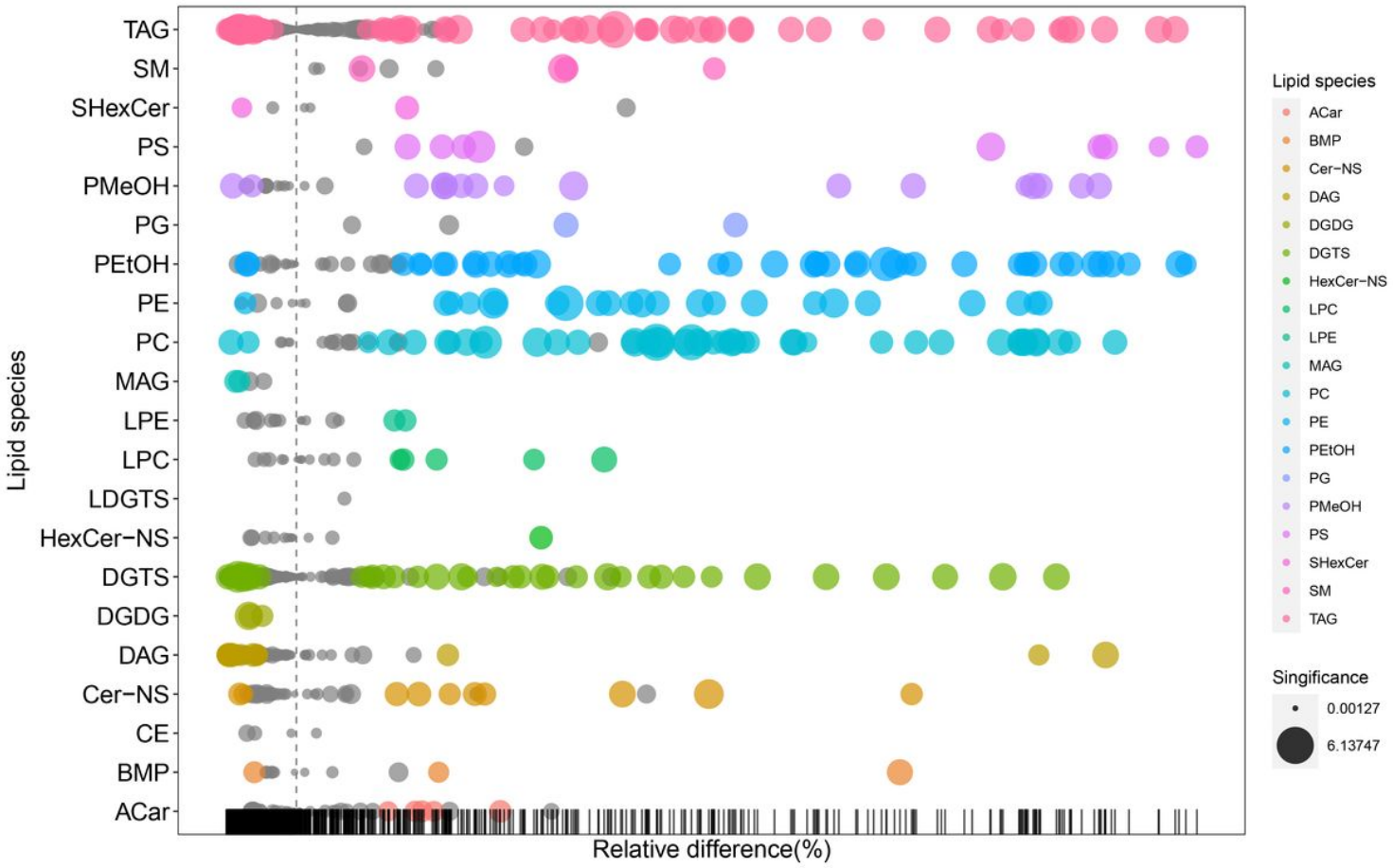

Figure 8

Bubble plot for the cancer group versus the para-cancer group.

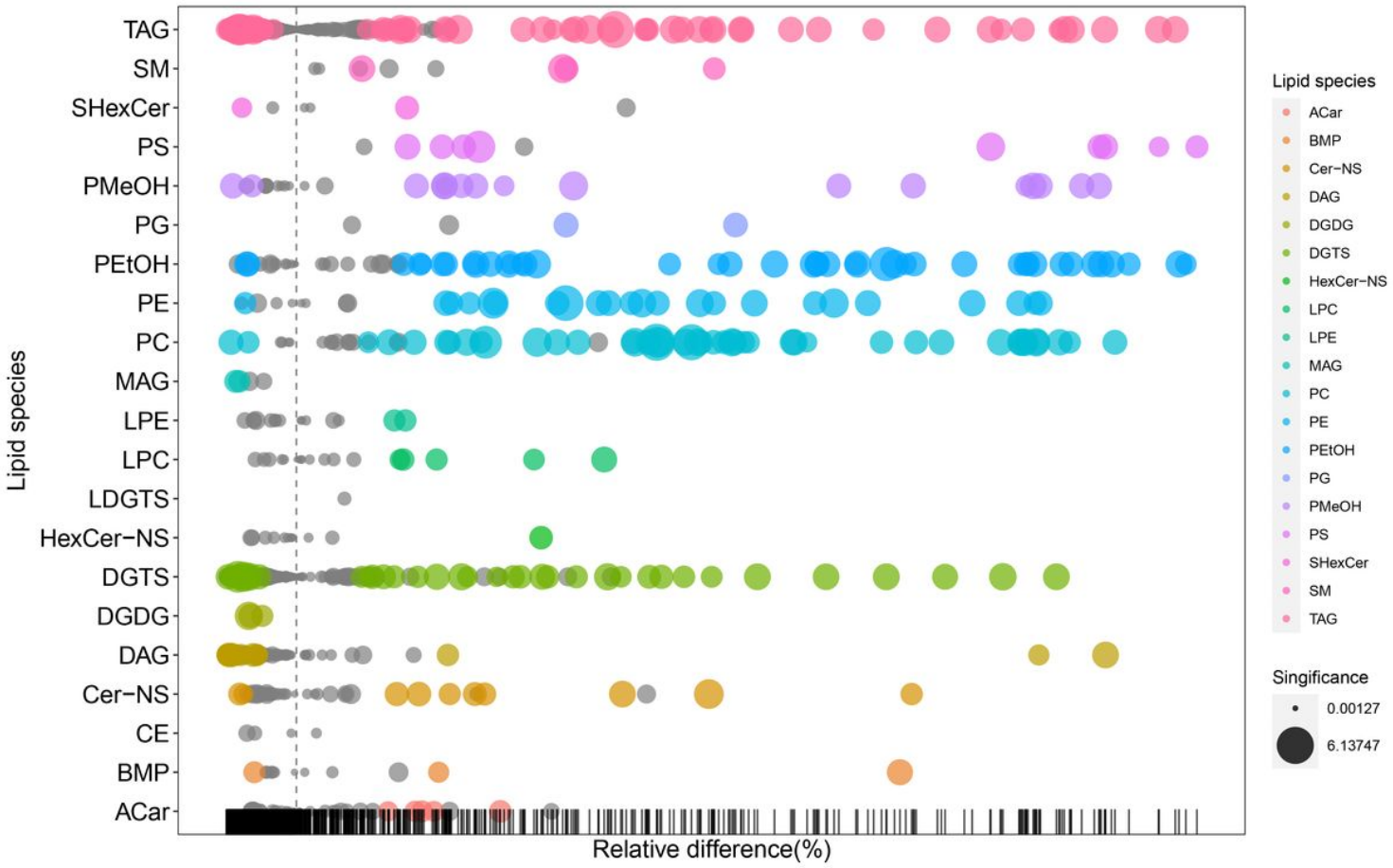

Figure 8

Bubble plot for the cancer group versus the para-cancer group.

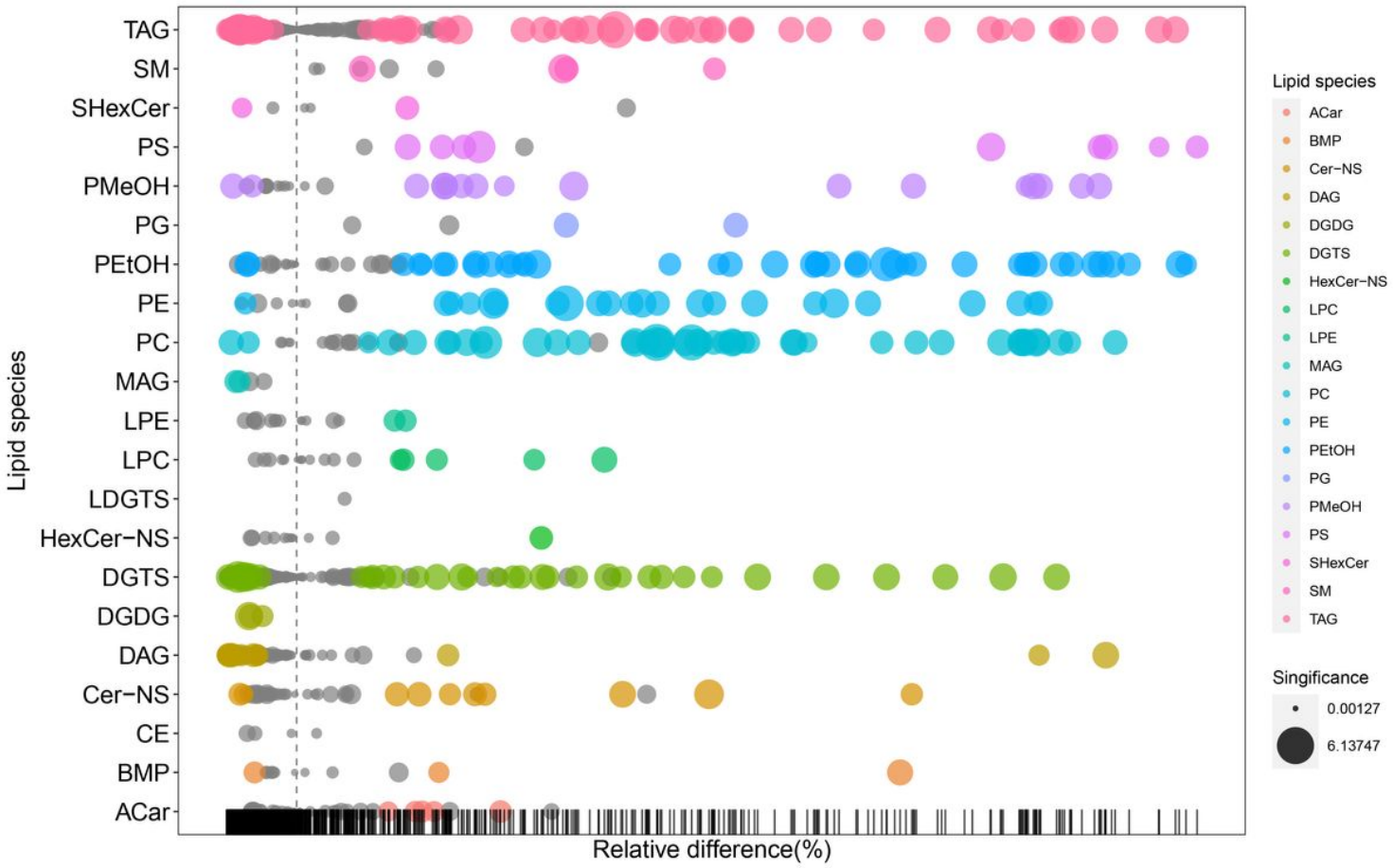

Figure 8

Bubble plot for the cancer group versus the para-cancer group.

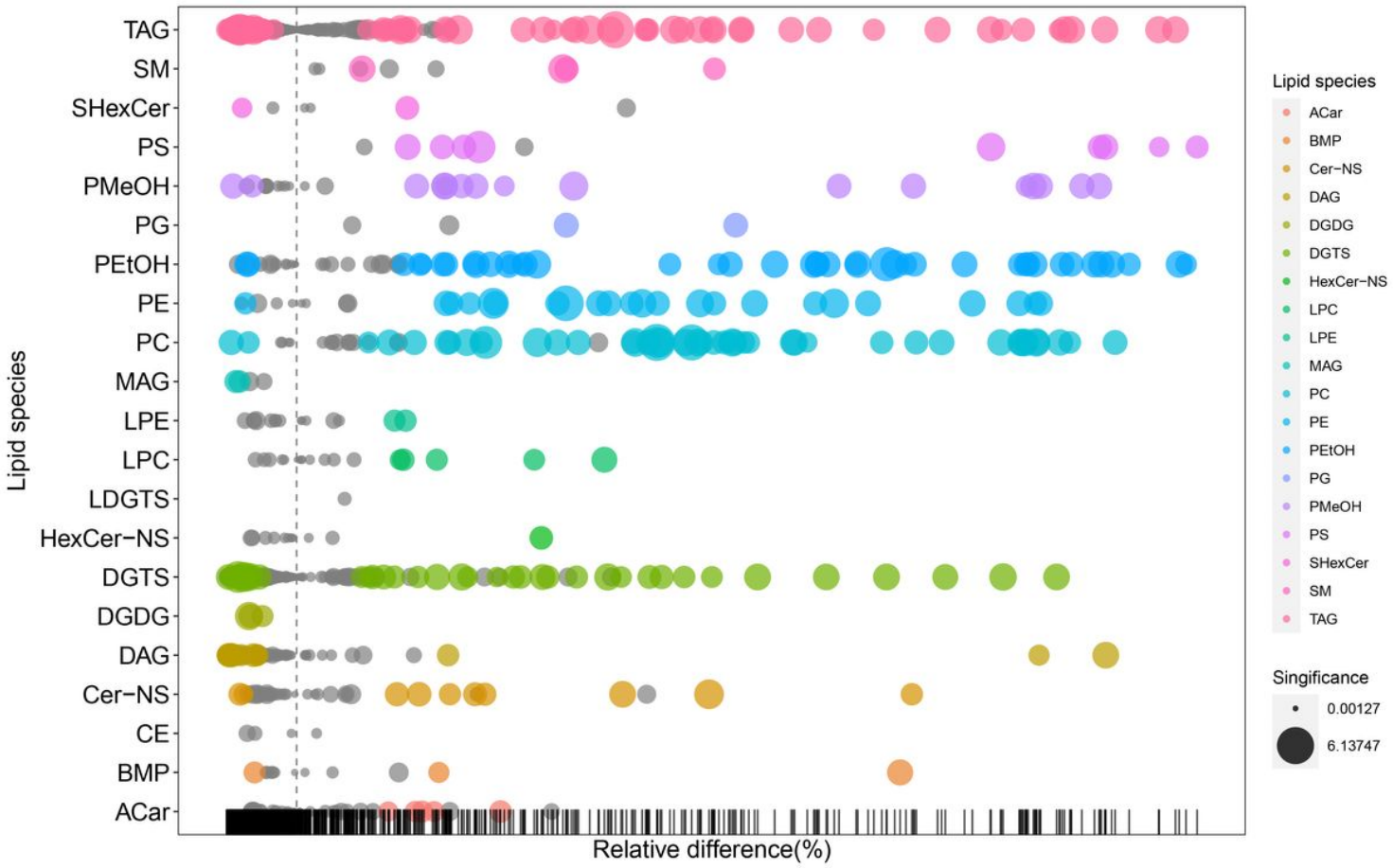

Figure 8

Bubble plot for the cancer group versus the para-cancer group.